

# Low background technologies for astroparticle experiments

A. Minamino (YNU) for  
K. Ichimura (Tohoku), M. Ikeda (ICRR), C. Ito (JAEA),  
Y. Iwata(JAEA), A. Takeda (ICRR), M. Tanaka (Waseda)

UGAP2024

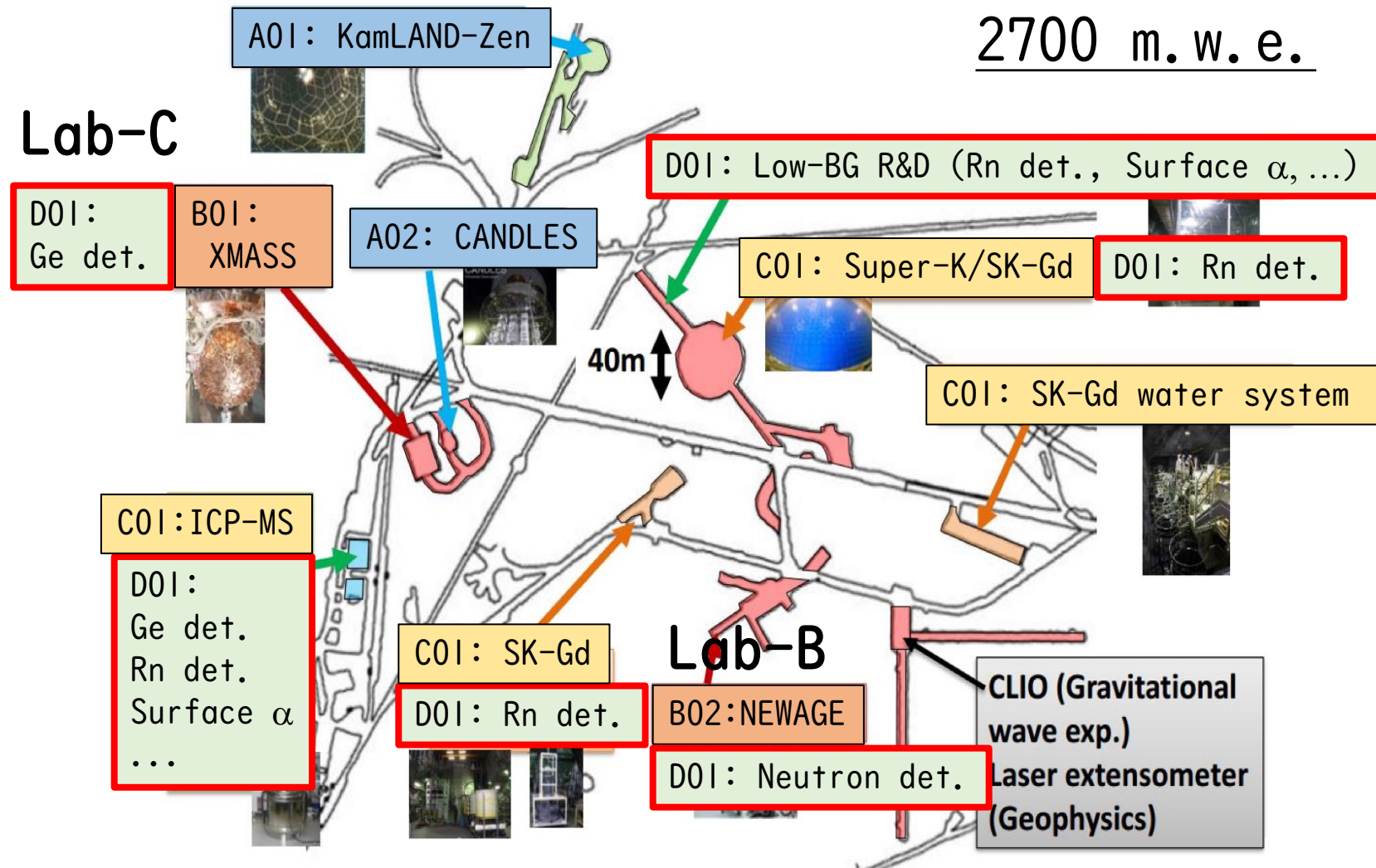
Mar. 6<sup>th</sup>, 2024

# Contents

- Kamioka Underground Laboratory
- Cooperation overview
- Material screenings with HPGe detectors
- Rn assay in  $\text{Gd}_2(\text{SO}_4)_3$  water
- Environmental neutron measurements in the underground
- Laser-induced emission spectroscopy for  $\text{Gd}^{3+}$
- Summary

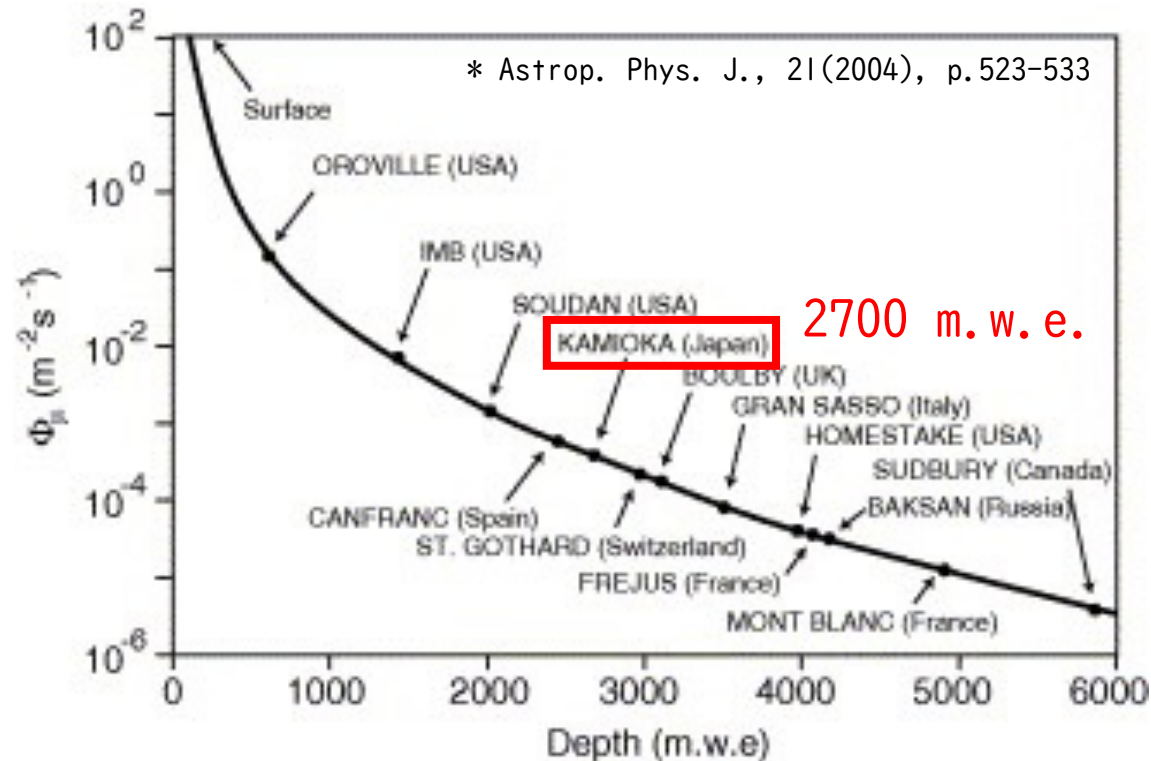
# Kamioka underground laboratory

# Kamioka Underground Laboratory

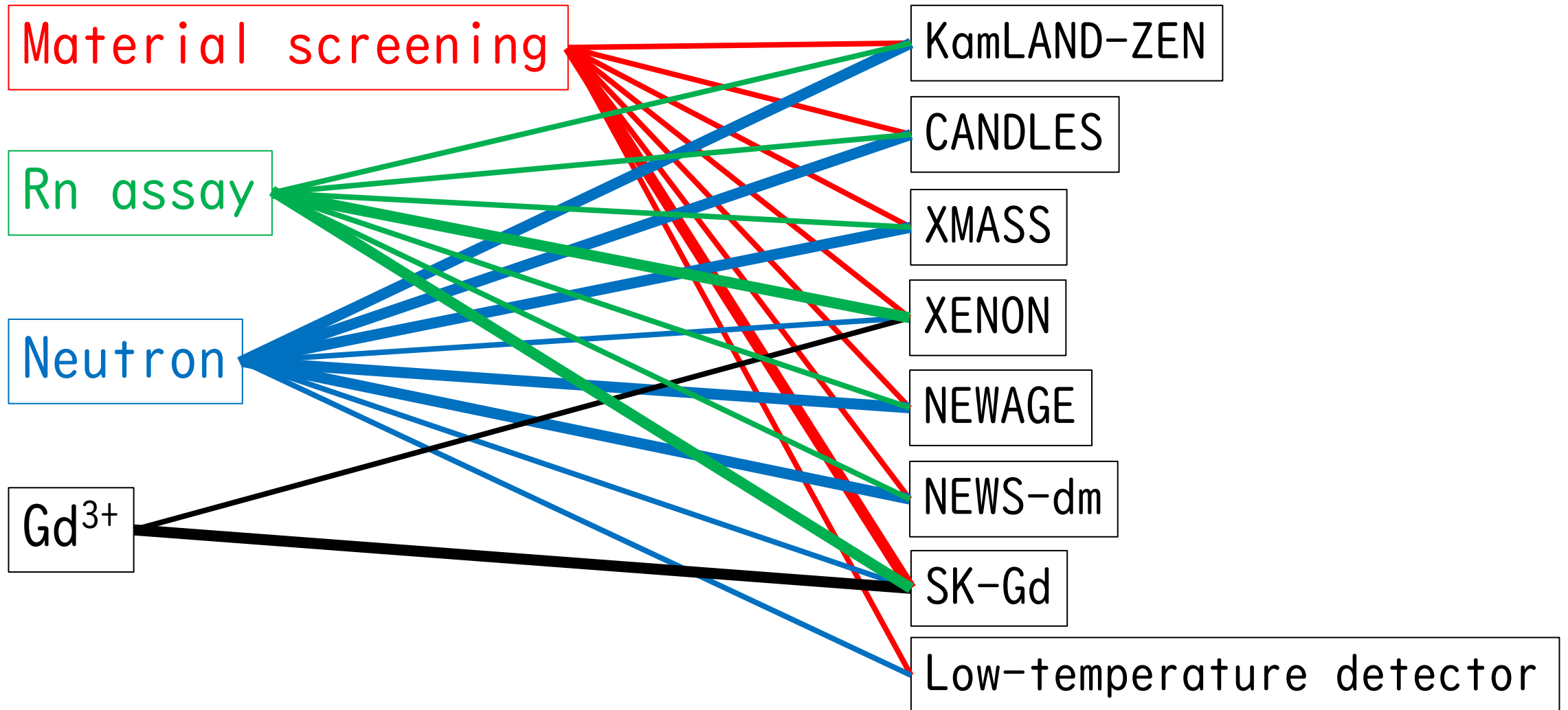


# Kamioka Underground Laboratory

- Cosmic ray  $\mu$  is  $10^{-5}$  times less than on the ground.
  - Cosmogenic radioactive nuclei & Neutrons originating from nuclear spallation due to cosmic ray  $\mu$  are suppressed.



# Cooperation overview

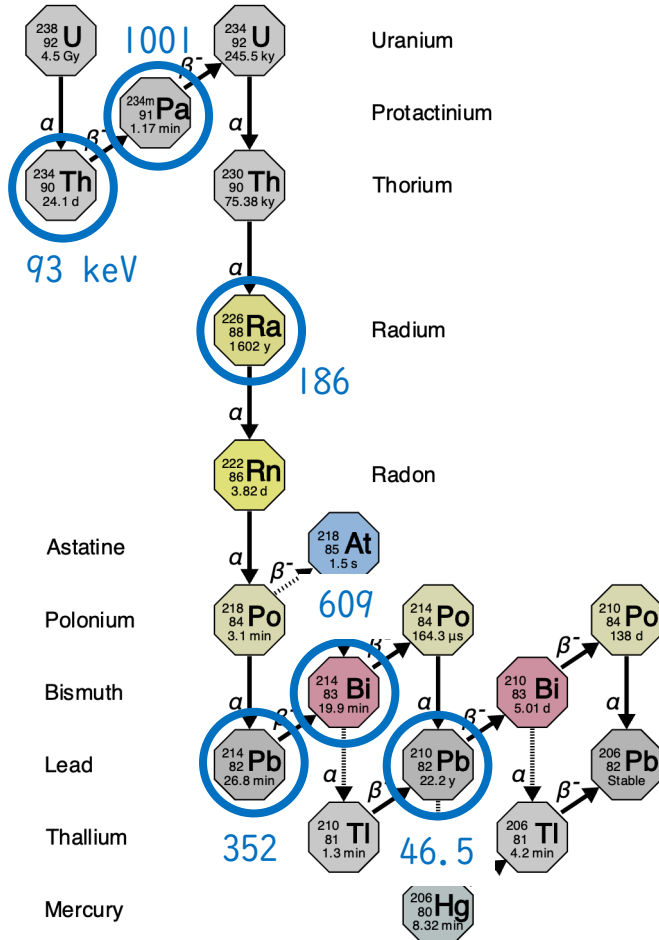


\*HPGe: High-Purity Germanium

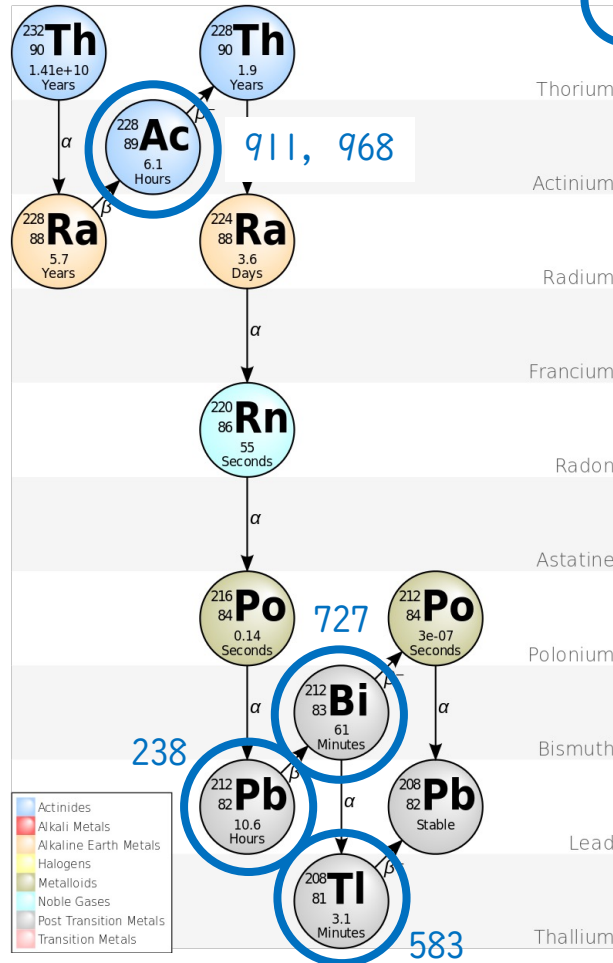
# Material screening with HPGe\* detectors

# Measurement using HPGe detectors

## Uranium series

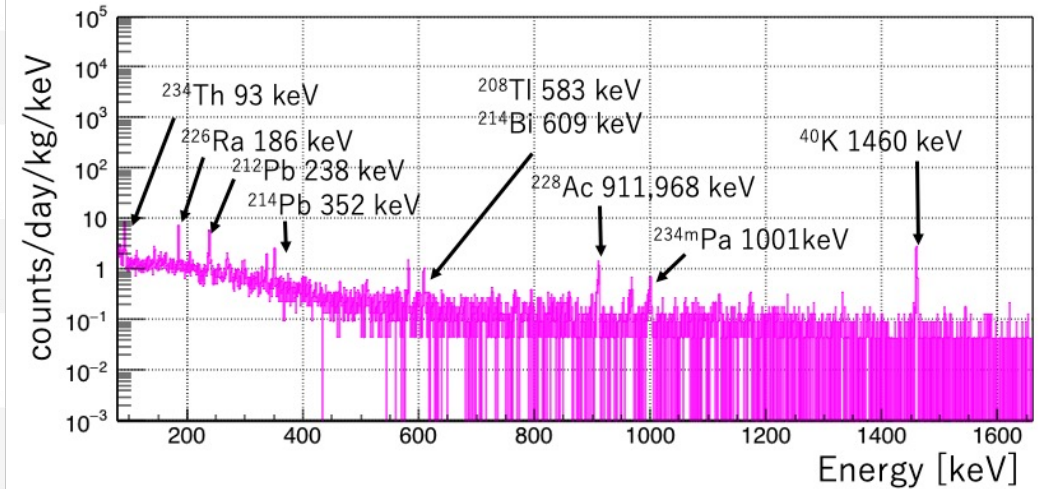


## Thorium series



- Nuclei whose gamma rays are detected by HPGe detectors
- The numbers are the energies of gamma rays (keV)

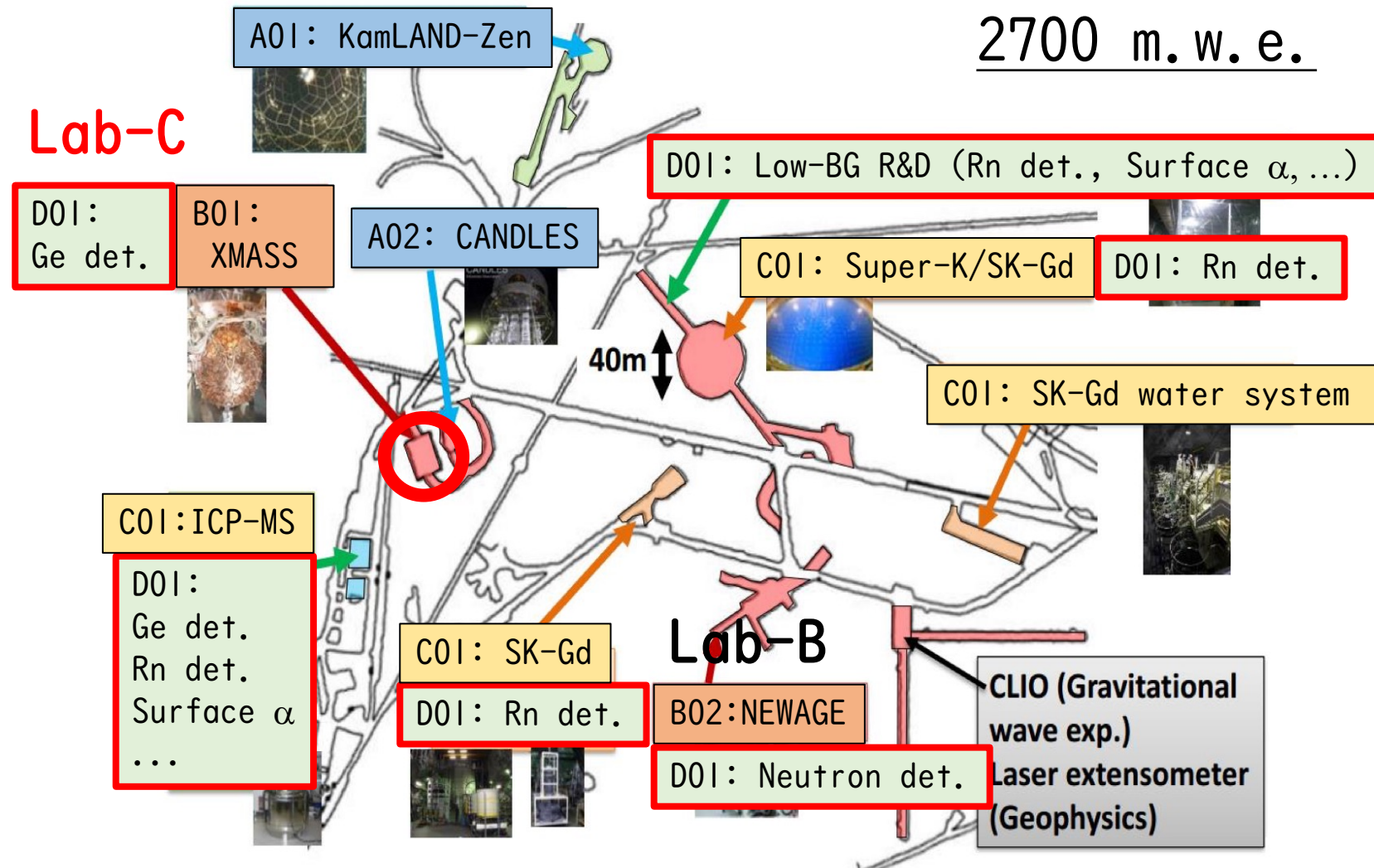
## Germanium detector background



Detector sensitivity depends on the background (Only a slight improvement even if measured for more than one month)



# Two HPGe detectors in Lab-C



# Two HPGe detectors in Lab-C

Ge01: Developed in XMASS collaboration  
Delivered in 2016



Ge02: Developed in this project (UGAP)  
Delivered in 2021

- P-type Coaxial HPGe detectors
  - Relative efficiency\*: >80%
  - Low background Aluminum endcap
  - Developed in collaboration with Mirion Technologies (T2FA series)
  - Transported from France to Japan by sea to prevent cosmogenic activation

\* Relative efficiency to a NaI(Tl) detector with a diameter & length of 3 inches for 1332.5 keV gamma total absorption peak from a  $^{60}\text{Co}$  point source placed 25 cm on the detector.

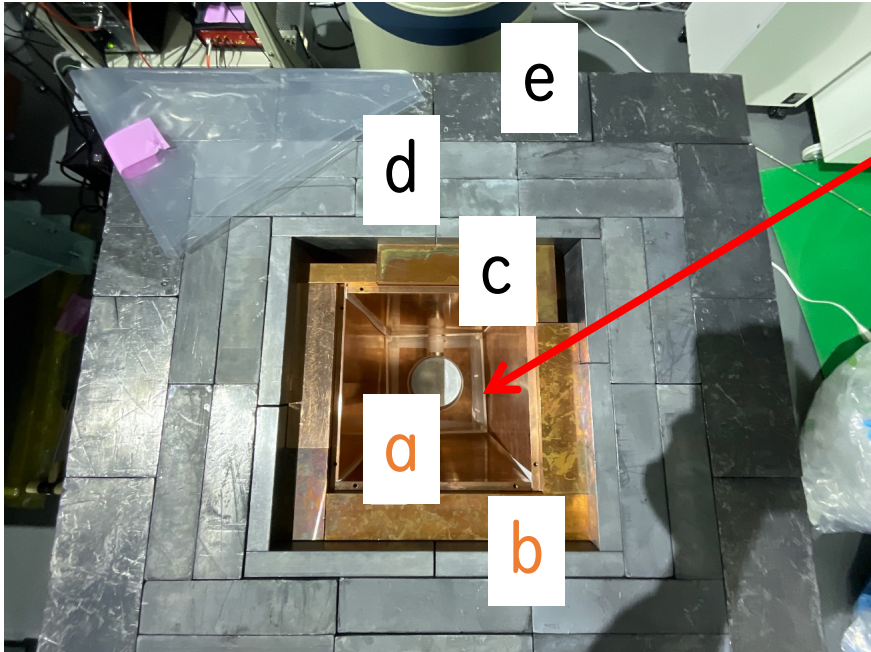
# Ge02: Photos at the time of delivery



## Performance

- Relative efficiency: 82.5%
- Energy resolution (FWHM)
  - 0.81 keV for 122 keV gammas ( $^{57}\text{Co}$ )
  - 1.74 keV for 1332 keV gammas ( $^{60}\text{Co}$ )

# Ge02: Radiation shield



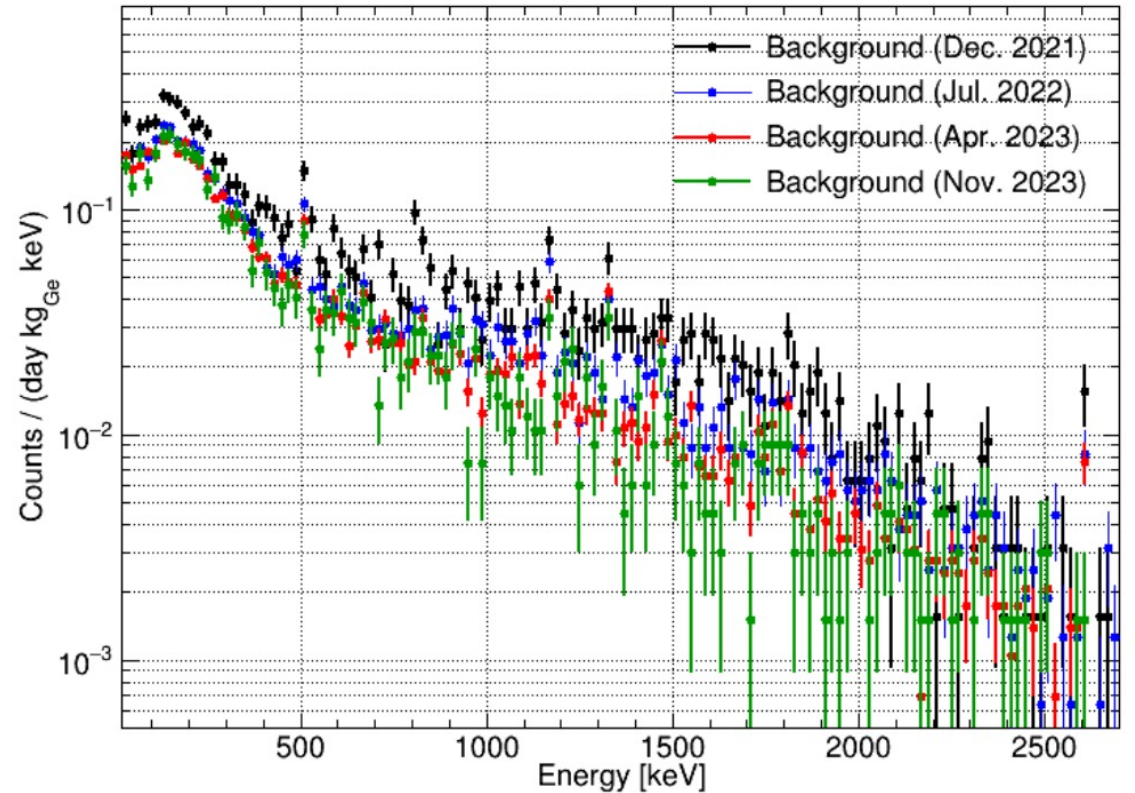
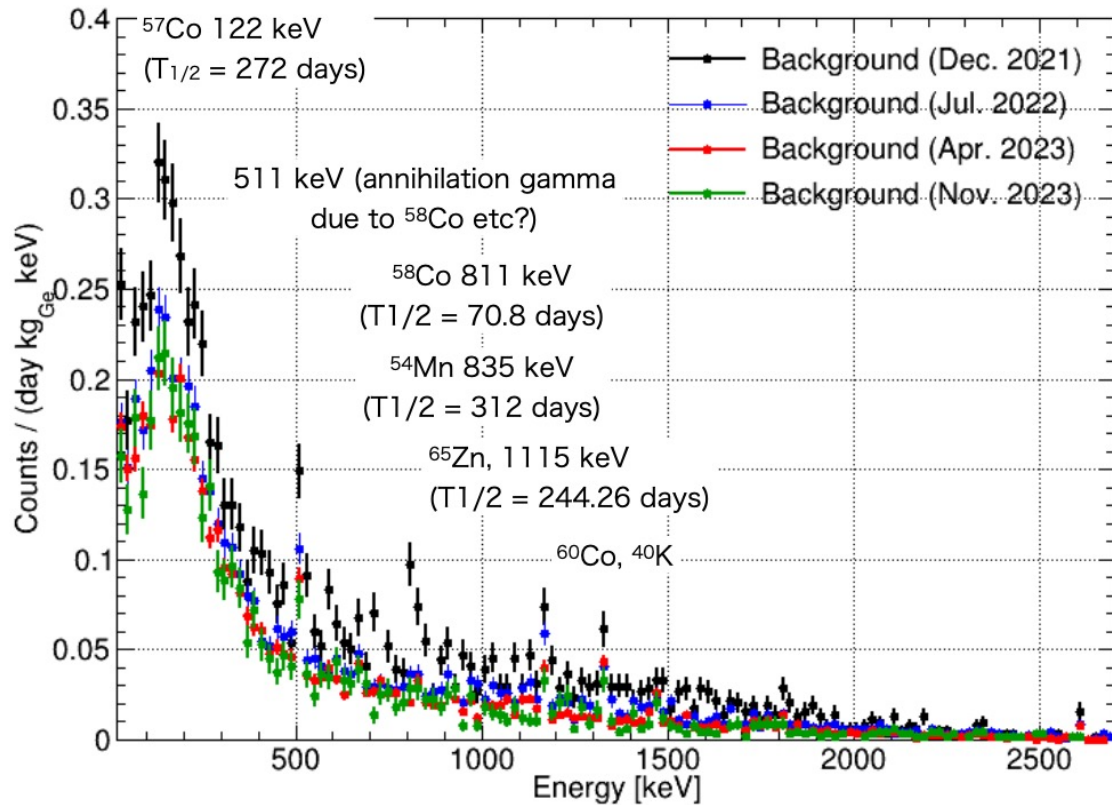
Sample space with **Rn free air**:  
capable of measuring 0 (10 kg)  
of gadolinium sulfate

- a: 1 cm 6N grade CU  
(surface etching with  $\text{HNO}_3^*$ )
- b: 5 cm OFHC Cu
- c: 2.5 cm Pb ( $^{210}\text{Pb}$ :  $5 \pm 3$  Bq/kg)  
(surface etching with  $\text{HNO}_3^*$ )
- d: 10 cm Pb ( $^{210}\text{Pb}$ :  $\sim 35$  Bq/kg)  
except for the top lid
- e: 10 cm Pb ( $^{210}\text{Pb}$ :  $\sim 180$  Bq/kg)



\* Surface etching with  $\text{HNO}_3$ :  
Soak in 4%  $\text{HNO}_3$  solution for 20 min.

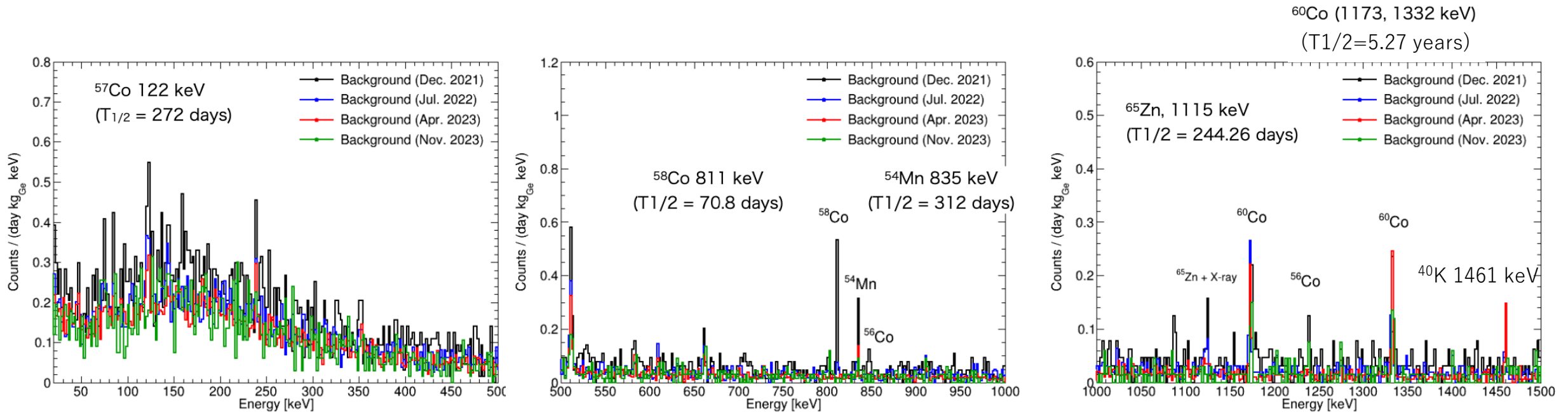
# Ge02: Background spectrum



## Count rate in 40-2700 keV:

$140.3 \pm 2.1$  cpd/kg<sub>Ge</sub> (Dec. 2021) → 
  $100.0 \pm 1.1$  cpd/kg<sub>Ge</sub> (Jul. 2022) → 
  $84.3 \pm 0.8$  cpd/kg<sub>Ge</sub> (Apr. 2023) → 
  $80.0 \pm 1.5$  cpd/kg<sub>Ge</sub> (Nov. 2023)

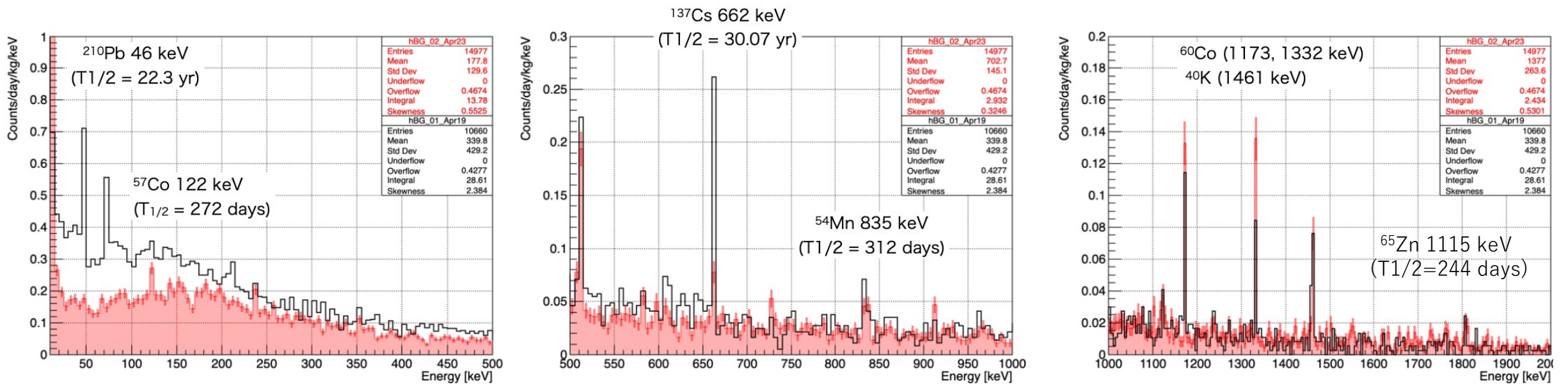
# Ge02: Background spectrum



Nucleus with relatively short half-lives are steadily decreasing.

# Background spectrum comparison between G01 and G02

Ge01: Oct. 2018 & Apr. 2019 (LT = 44 days), Ge02: Apr.-Jul. 2023 (LT = 86 days)



## Count rate in 40–2700 keV:

Ge01:  $140.3 \pm 2.1$  cpd/kg<sub>Ge</sub> → Ge02:  $84.3 \pm 0.8$  cpd/kg<sub>Ge</sub> (30% improvement)

- <sup>137</sup>Cs and <sup>210</sup>Pb peaks have been dramatically improved.
- Continuous components below 600 keV have also been improved.

# Ge01 & Ge02: Background spectrum

<https://doi.org/10.1093/ptep/ptad136>

| Detector  | Ge01            | Ge02            |                 |                 |                 |
|---|-----------------|-----------------|-----------------|-----------------|-----------------|
| Date  | Dec. 2019       | Dec. 2021       | Jul. 2022       | Apr. 2023       | Nov. 2023       |
| Measurement time (d)  | 23.0            | 19.0            | 47.2            | 86.2            | 19.9            |
| Count rate ( $\text{kg}_{\text{Ge}}^{-1} \text{day}^{-1}$ ) |                 |                 |                 |                 |                 |
| Integral 40 – 2700 keV                                      | 112.6           | 140.2           | 100.0           | 84.3            | 80.0            |
| $^{208}\text{Tl}$ , 2614 keV                                | $0.08 \pm 0.04$ | $0.25 \pm 0.09$ | $0.16 \pm 0.05$ | $0.13 \pm 0.03$ | $0.03 \pm 0.03$ |
| $^{214}\text{Bi}$ , 609 keV                                 | $0.39 \pm 0.10$ | $0.25 \pm 0.09$ | $0.38 \pm 0.07$ | $0.23 \pm 0.04$ | $0.24 \pm 0.08$ |
| $^{60}\text{Co}$ , 1333 keV                                 | $0.41 \pm 0.10$ | $0.66 \pm 0.14$ | $0.48 \pm 0.08$ | $0.68 \pm 0.07$ | $0.48 \pm 0.12$ |
| $^{40}\text{K}$ , 1461 keV                                  | $0.44 \pm 0.11$ | $0.31 \pm 0.10$ | $0.44 \pm 0.07$ | $0.42 \pm 0.05$ | $0.18 \pm 0.07$ |
| $^{137}\text{Cs}$ , 662 keV                                 | $1.29 \pm 0.18$ | $0.53 \pm 0.13$ | $0.38 \pm 0.07$ | $0.32 \pm 0.05$ | $0.42 \pm 0.11$ |
| $^{210}\text{Pb}$ , 46.5 keV                                | $3.24 \pm 0.29$ | $0.69 \pm 0.14$ | $0.64 \pm 0.09$ | $0.59 \pm 0.06$ | $0.27 \pm 0.09$ |

Nuclei have relatively short half-lives are steadily decreasing.



# G02: Comparison with HPGe detectors around the world

<https://doi.org/10.1093/ptep/ptad136>

| Site  | Detector                 | Crystal mass [kg] | Relative efficiency [%] | FWHM at 1333 keV [keV] | BG rate 60 – 2700 keV [ $\text{kg}_{\text{Ge}}^{-1} \text{d}^{-1}$ ] |
|-------|--------------------------|-------------------|-------------------------|------------------------|--|
| Japan | Kamioka Ge02 (This work) | 1.68              | 80                      | 1.82                   | <b>81.3±0.7</b>  |
|       | Ge01 [2]                 | 1.68              | 80                      | 2.39                   | 104.5  |
| Italy | LNGS Gator [16]          | 2.2               | 100.5                   | 1.98                   | 89.0±0.7   |
|       | GeMPI [16]               | 2.2               | 98.7                    | 2.20                   | <b>24±1</b>  |
| UK    | BUGS Belmont [2]         | 3.2               | 160                     | 1.92                   | 90.0   |
|       | Merrybent [2]            | 2.0               | 100                     | 1.87                   | 145.0  |
| Spain | LSC GeOroel [2]          | 2.31              | 109                     | 2.22                   | 128.7  |
|       | Asterix [2]              | 2.13              | 95.1                    | 1.92                   | 171.3  |
|       | GeAnayet [2]             | 2.26              | 109                     | 1.99                   | 461.2  |
| US    | BHUC Maeve [17]          | 2.0               | 85                      | 3.19                   | 956.1  |
| Swiss | LVdA GeMSE [16,18]       | 2.0               | 107.7                   | 1.96                   | 88±1   |

We have developed an ultra-low BG HPGe detector with the world's highest level of sensitivity.

# G02: Comparison with HPGe detectors around the world

[\\*STELLA at LNGS, TAUP2023](#)

| detector | total and peak background count rate [ $\text{d}^{-1} \text{kg}^{-1}_{\text{Ge}}$ ] |                 |                 |                 |
|----------|---|-----------------|-----------------|-----------------|
|          | 40-2700 keV   | 352 keV         | 583 keV         | 1461 keV        |
| GeMi     | $555 \pm 7$   | $4.1 \pm 1.0$   | $1.4 \pm 0.5$   | $6.1 \pm 0.8$   |
| GePV     | $498 \pm 5$   | $2.6 \pm 0.7$   | $1.8 \pm 0.4$   | $3.2 \pm 0.4$   |
| GsOr     | $442 \pm 5$   | $2.0 \pm 0.5$   | $0.76 \pm 0.35$ | $4.2 \pm 0.5$   |
| GePaolo  | $222 \pm 2$   | $1.1 \pm 0.3$   | $0.31 \pm 0.16$ | $1.8 \pm 0.2$   |
| GeCris   | $115 \pm 2$   | $0.29 \pm 0.22$ | $< 0.13$        | $0.88 \pm 0.22$ |
| GeMPI    | $71 \pm 2$  | $< 0.07$        | $< 0.06$        | $0.24 \pm 0.03$ |

Ge02       $84 \pm 1$        $0.44 \pm 0.05$        $0.25 \pm 0.04$        $0.42 \pm 0.05$

We have developed an ultra-low BG HPGe detector with the world's highest level of sensitivity.

# Gd<sub>2</sub>(SO<sub>4</sub>)<sub>3</sub> screening for SK-Gd

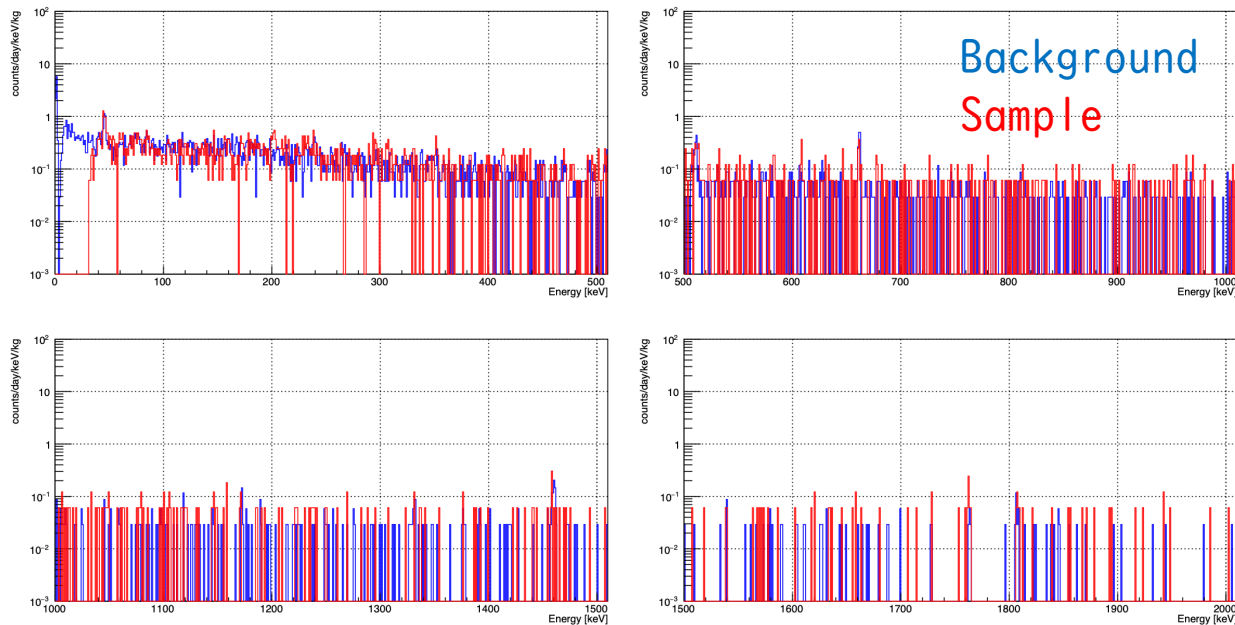
- Gd<sub>2</sub>(SO<sub>4</sub>)<sub>3</sub> dissolved in Super-Kamiokande
  - 13 tons in 2020
  - 26 tons in 2022
- Requirements for RI in Gd<sub>2</sub>(SO<sub>4</sub>)<sub>3</sub> for SK-Gd

| Chain             | Isotope           | Criterion [mBq/kg] | Physics target |
|-------------------|-------------------|--------------------|----------------|
| <sup>238</sup> U  | <sup>238</sup> U  | < 5                | SRN            |
|                   | <sup>226</sup> Ra | < 0.5              | Solar          |
| <sup>232</sup> Th | <sup>232</sup> Th | < 0.05             | Solar          |
|                   | <sup>228</sup> Ra | < 0.05             | Solar          |

- Select an appropriate method for each nucleus
  - <sup>238</sup>U, <sup>232</sup>Th: ICP-MS
  - **Other nuclei: HPGe detector**

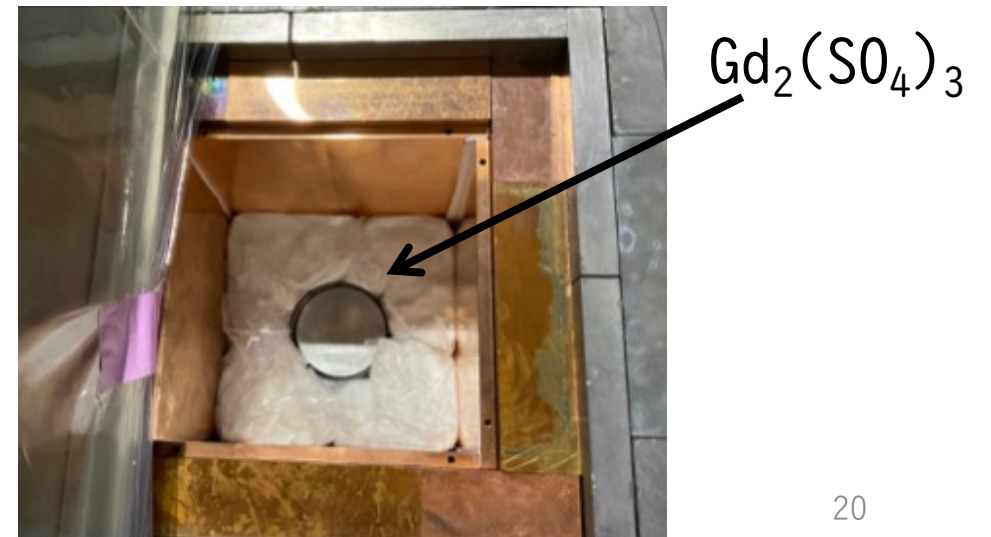
# $Gd_2(SO_4)_3$ screening with HPGe

- In 2022, 26 tons of  $Gd_2(SO_4)_3$  dissolved in SK-Gd was delivered in 37 lots.
  - HPGe detector measurements were performed on 34 lots using Ge01 & G02. The other lots were measured by European collaborators.



Typical spectrum of  $Gd_2(SO_4)_3$  screening

20 days required to measure each lot



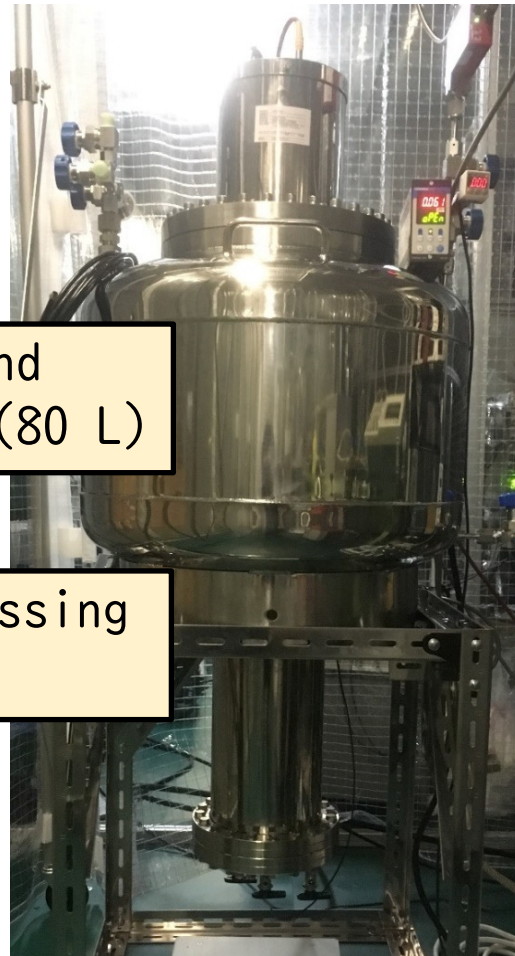
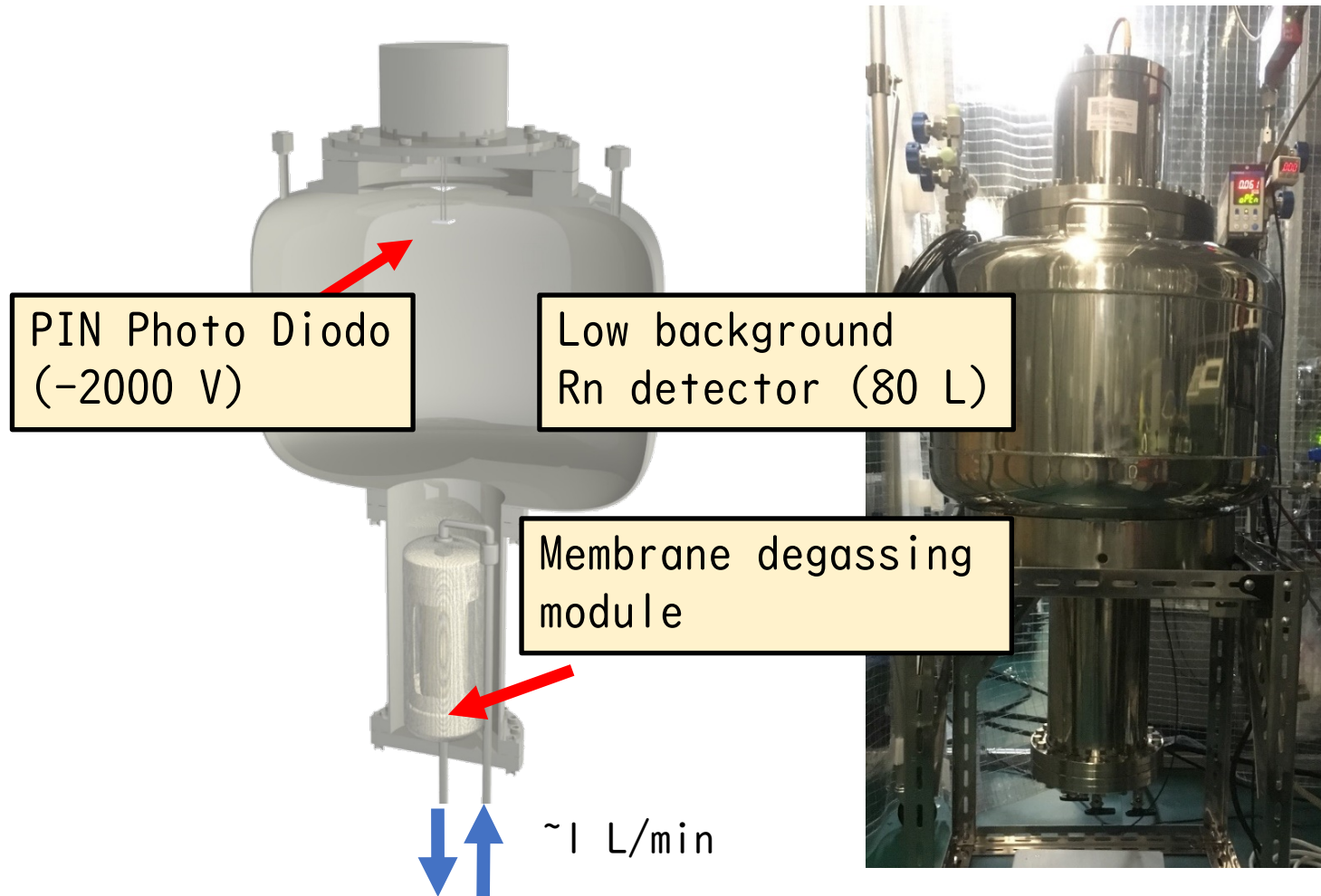
Rn assay in  $\text{Gd}_2(\text{SO}_4)_3$   
water

# Continuous measurement of $^{222}\text{Rn}$ in $\text{Gd}_2(\text{SO}_4)_3$ water

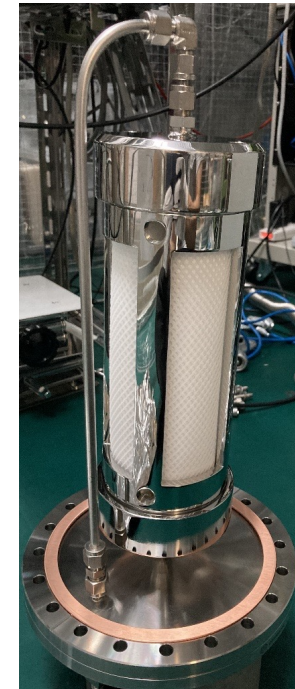
- Motivation
  - SK-Gd:  $\beta$ -decay of  $^{214}\text{Bi}$  in the  $^{222}\text{Rn}$  daughter nucleus becomes a background in solar neutrino observation.
  - XENONnt:  $^{222}\text{Rn}$  affects the dead time of neutron veto water Cerenkov detector.
- Required sensitivity
  - The background is  $<1 \text{ mBq/m}^3$ .
- Development policy
  - Improve the existing water radon detector\*.

\* C. Mitsuda et al., NIMA 497 (2003) 414.

# Continuous measurement of $^{222}\text{Rn}$ in $\text{Gd}_2(\text{SO}_4)_3$ water

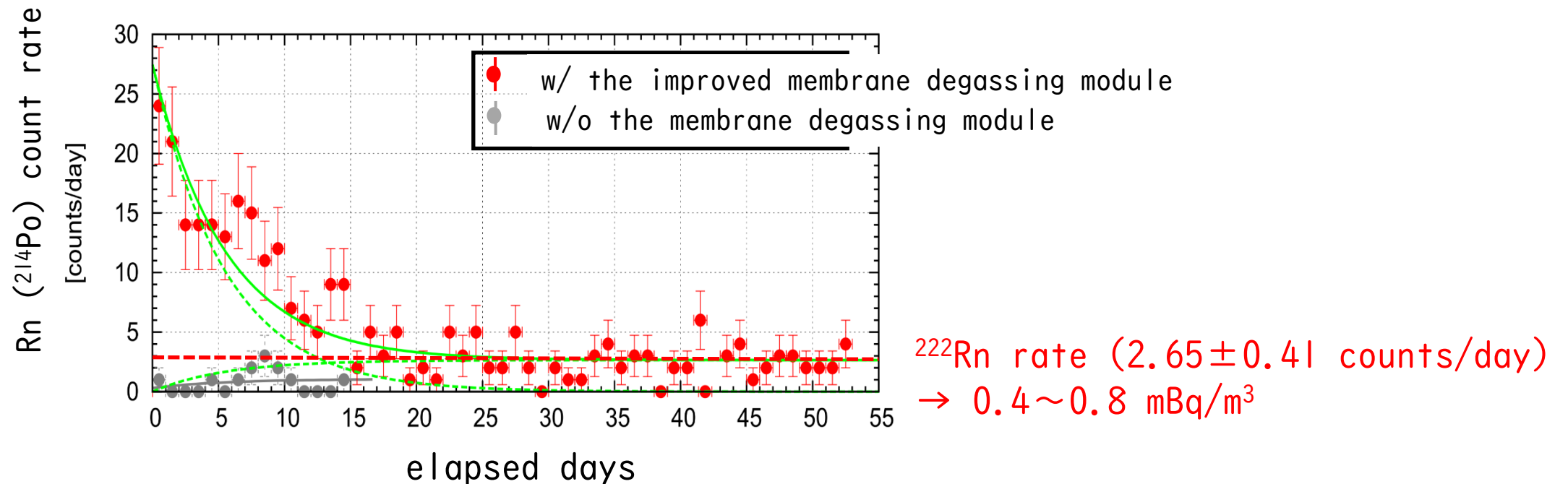


- The membrane degassing module is the main background source.
- Housing changed from resin to stainless steel.



# Continuous measurement of $^{222}\text{Rn}$ in $\text{Gd}_2(\text{SO}_4)_3$ water

- We achieved the required background level of  $<1$  mBq/m $^3$ .
  - 10x improvement from the past design.



- Four detectors are started operation in SK-Gd & XENONnT.



# Automation of high-sensitivity $^{222}\text{Rn}$ measurement in $\text{Gd}_2(\text{SO}_4)_3$ water

- High-sensitivity measurement method
  - After adsorbing  $^{222}\text{Rn}$  onto activated carbon cooled to  $-75^\circ\text{C}$ , the activated carbon is heated to  $150^\circ\text{C}$  to release  $^{222}\text{Rn}$ .
  - Then,  $^{222}\text{Rn}$  is measured using a low-background radon detector.
- Problems with the conventional method
  - Complex valve operations had to be performed manually.
  - It was necessary to attach and detach the refrigerator and heater when cooling and heating the activated carbon.
- Goal
  - Automation of work with remote valves, temperature controller, and operation panel.

# Automation of high-sensitivity $^{222}\text{Rn}$ measurement in $\text{Gd}_2(\text{SO}_4)_3$ water

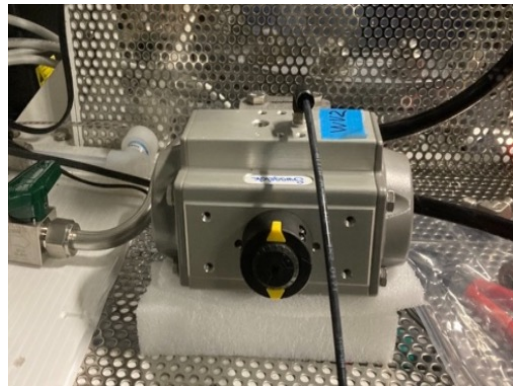
- Newly introduced equipment

## Remote valves

for pure air



for  $\text{Gd}_2(\text{SO}_4)_3$  water



## Temp. controller

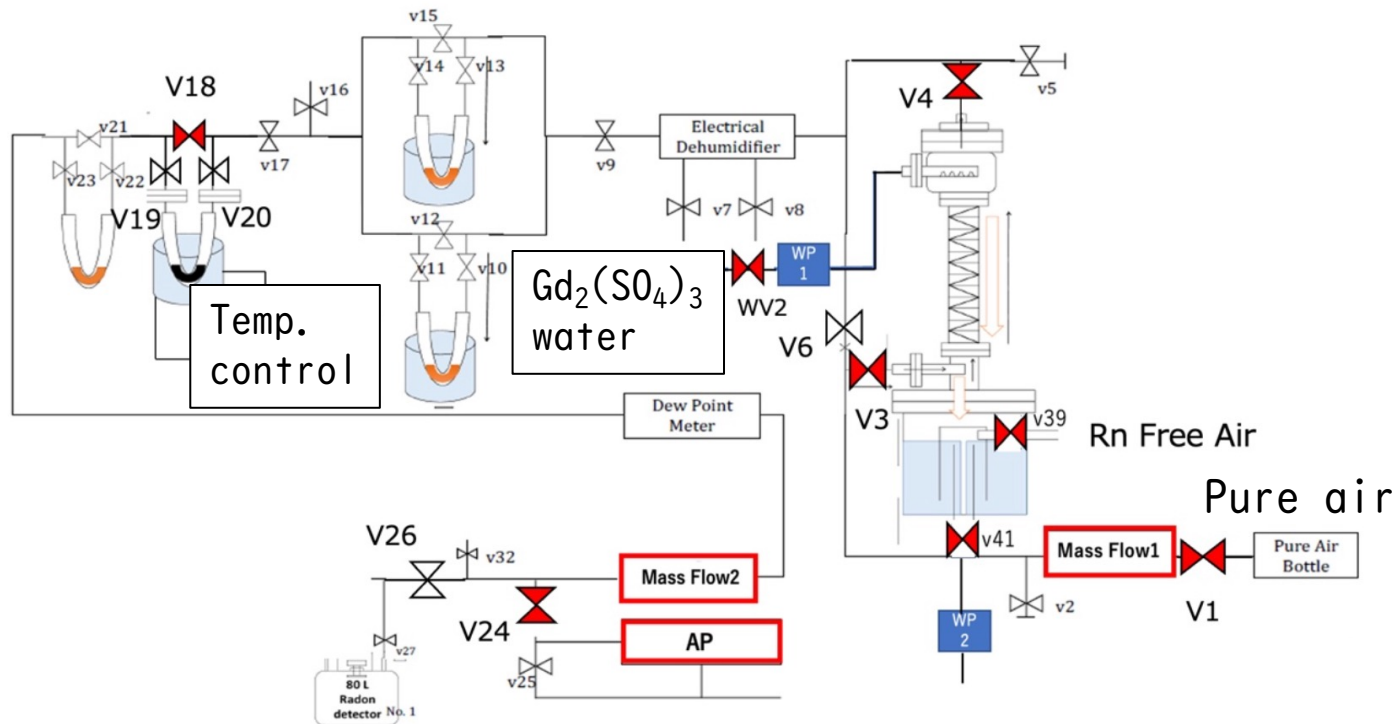
-75°C to 150°C



## Operation panel



# Automation of high-sensitivity $^{222}\text{Rn}$ measurement in $\text{Gd}_2(\text{SO}_4)_3$ water



| Rn concentration measurement |  |  |                     |
|------------------------------|--|--|---------------------|
|                              | Preparation  | Unistat → -60°C  | Concentration       |
| V1                           |  |  |                     |
| V3                           |  |  |                     |
| V4                           |  |  |                     |
| V6                           |  |  |                     |
| WP2                          |  |  |                     |
| V41                          |  |  |                     |
| V18                          |  |  |                     |
| V19                          |  |  |                     |
| V20                          |  |  |                     |
| V24                          |  |  | 10 sec delayed open |
| V26                          |  |  |                     |
| V39                          |  |  |                     |
| Mass Flow1                   |  | 2.00L(Default)   |                     |
| Mass Flow2                   |  | 2.00L(Default)   |                     |
| AP                           |  |  | 10 sec delayed open |
| WP1                          | 30 sec delayed open  |  |                     |
| WP2                          | When WP delayedtimer1 finishes to count                                      |  |                     |
| WP delayedtimer1             | Counting until the set delayed time is reached                               |  |                     |
| WP delayedtimer2             |  |  |                     |
| Unistat                      | Cooling to -80°C   | -60°C to -80°C   | -80°C               |
| Delay timer1                 |  | Counting   |                     |
| Delay timer2                 |  |  |                     |
| Delay timer4                 |  |  |                     |
| Remarks                      | Insert delayed time into "Drain WP delayed timer at Step 1" in Timer Monitor | Insert delayed time into "Delayed timer of starting Step 2" in Timer Monitor |                     |

Yellow box : Open

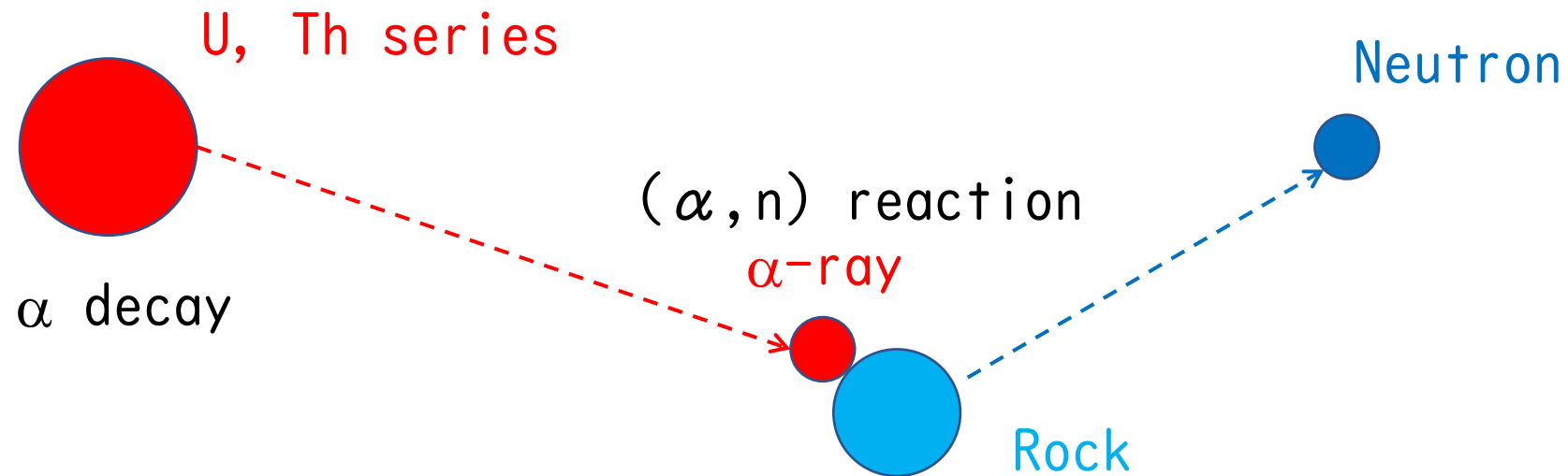
Orange box : Open when conditions

We have successfully automated the work.  
The system will start operation in SK-Gd.

Environmental neutron  
measurements  
in the underground

# The primary sources of environmental neutrons in the underground

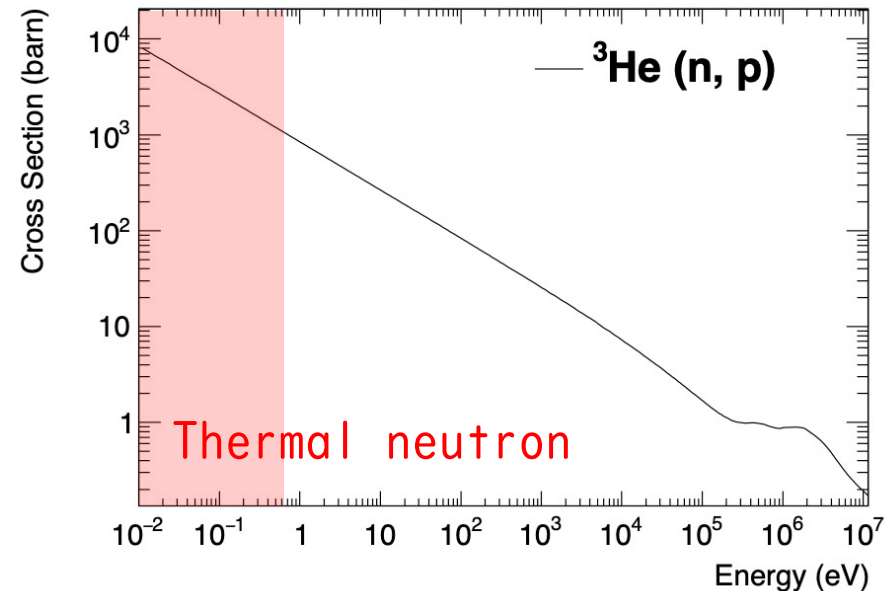
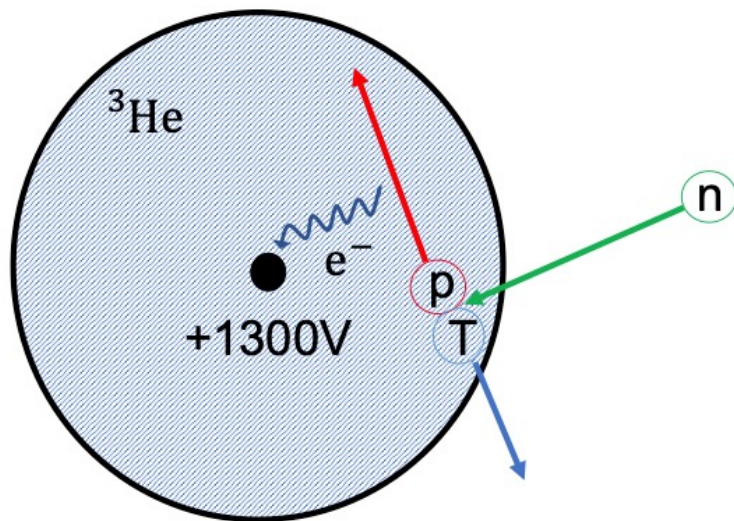
- $(\alpha, n)$  reaction between rock and  $\alpha$ -rays generated by the decay of the U and Th series contained therein.



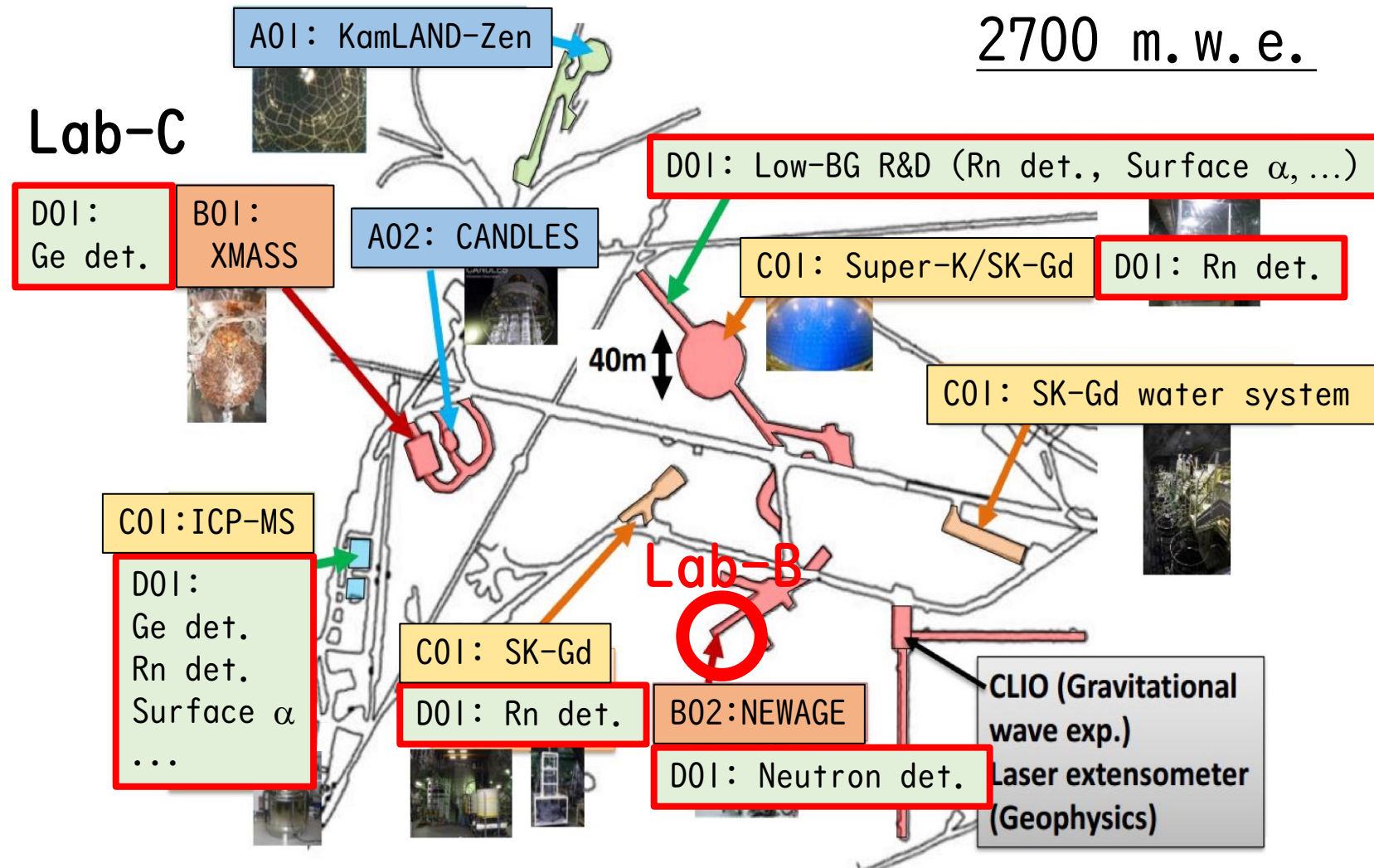
$^3\text{He}$  proportional counter

# $^3\text{He}$ proportional counter

- $^3\text{He} + n \rightarrow p + T + 0.765 \text{ MeV}$
- High sensitivity to thermal neutrons
- Fast neutrons are measured after decelerating using a moderator (such as polyethylene).



# Environmental neutron measurement in Lab-B

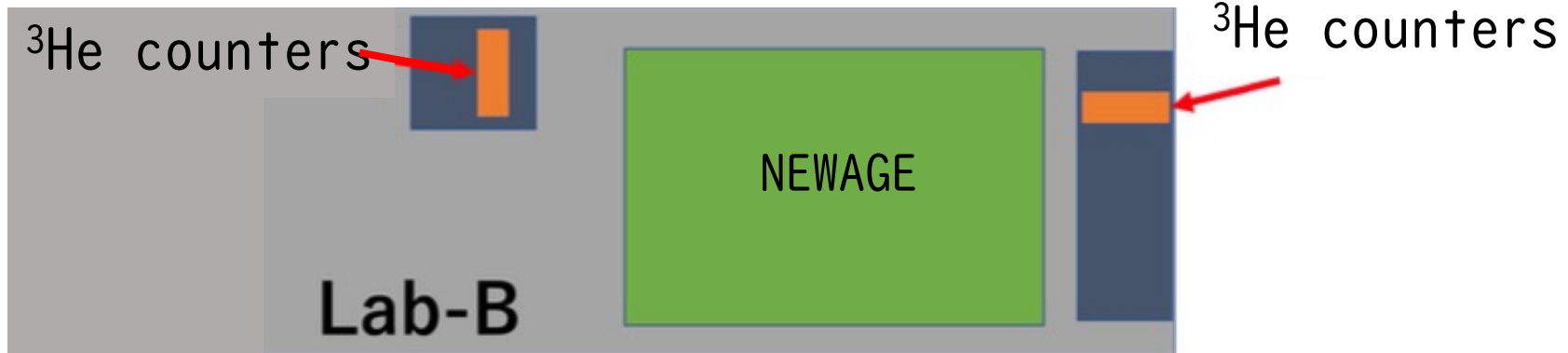




# Two $^3\text{He}$ proportional counters in Lab-B

Jul. 2021 ~ Apr. 2023

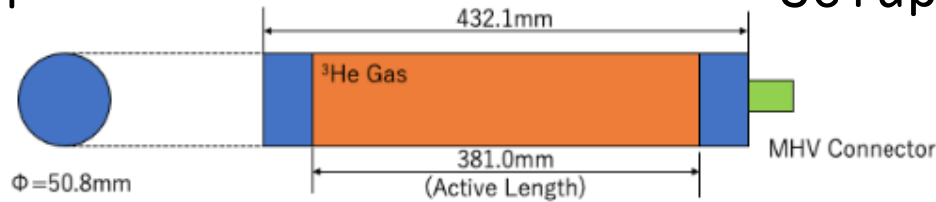
Apr. 2023 ~



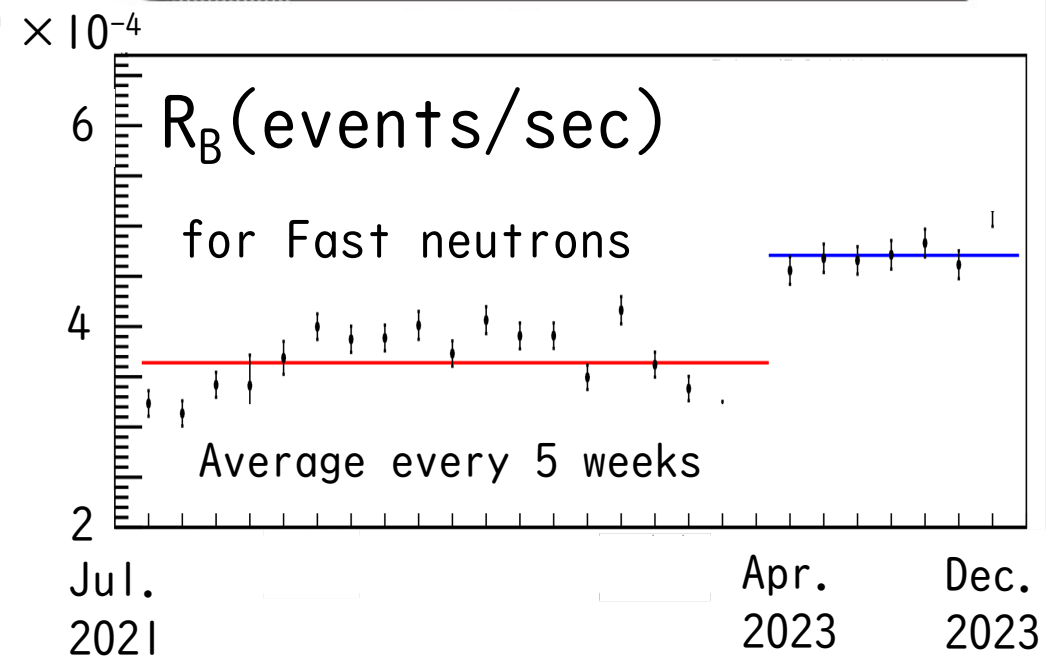
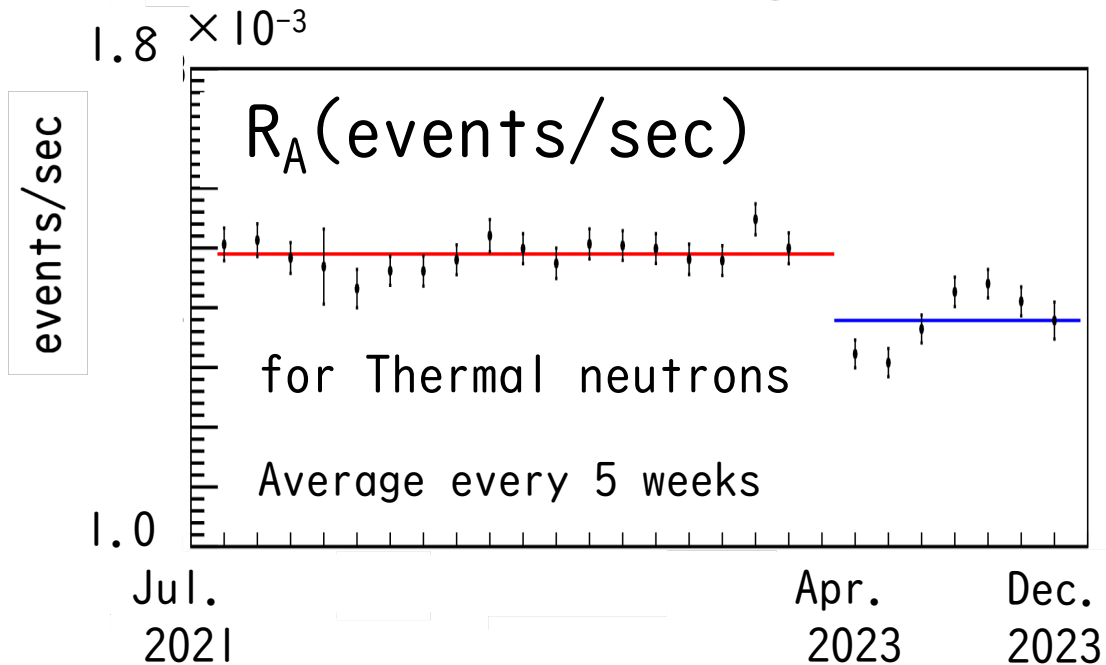
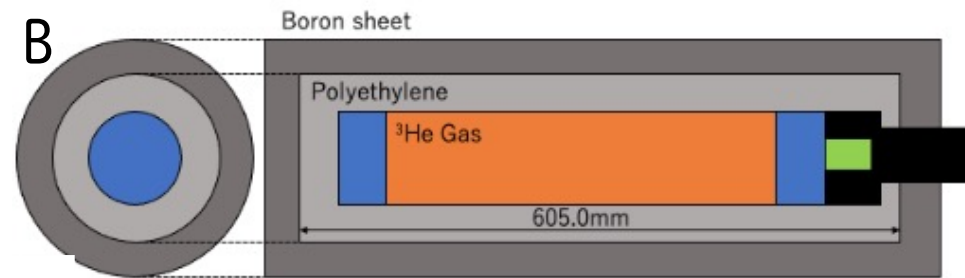
# Environmental neutron measurement in Lab-B with two $^3\text{He}$ proportional counters

- Jul. 2021 ~ Apr. 2023, Apr. 2023 ~

Setup A



Setup B



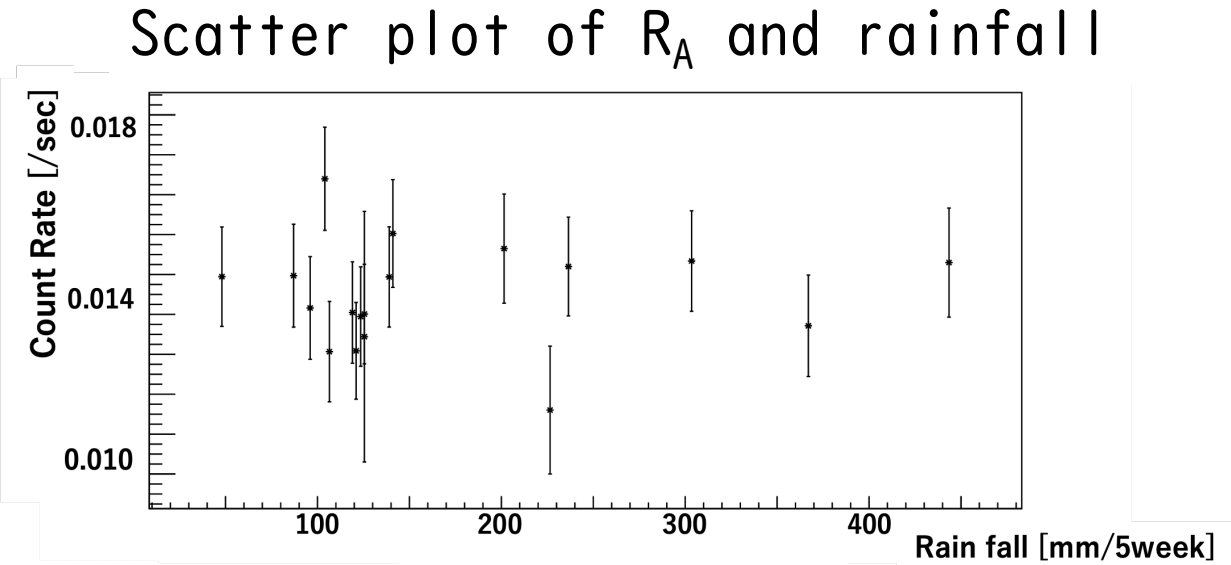
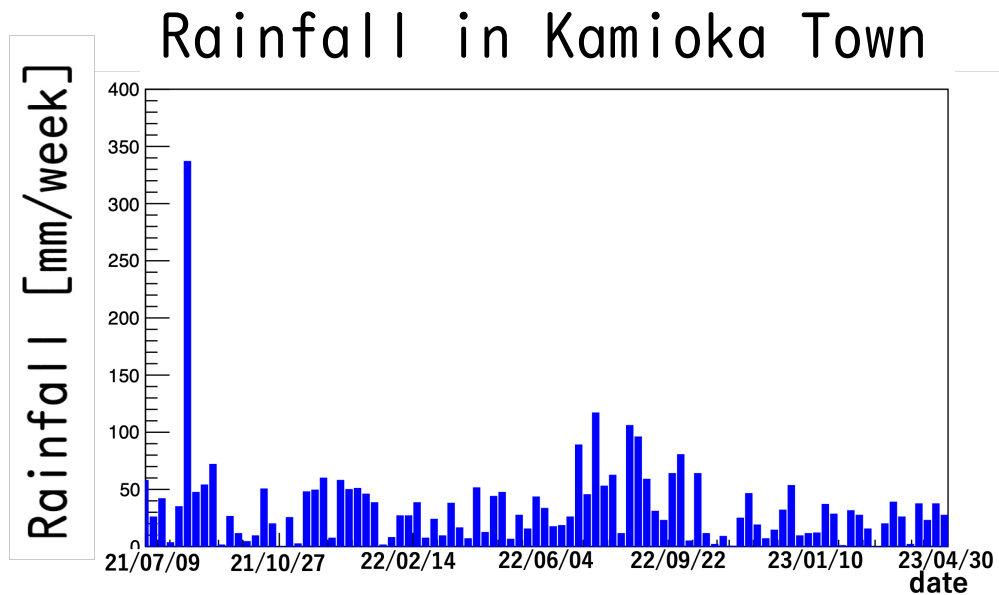
# Correlation between Lab-B neutron flux and environmental parameters

We investigated the correlation between Lab-B neutron flux and environmental parameters from Jul. 2021 to Apr. 2023.

1. Rainfall
2. Rn concentration in the mine-tunnel air
3. Humidity in the mine-tunnel air

# Correlation with Rainfall

- Using rainfall data observed in Kamioka Town (~12 km from the Kamioka underground laboratory.)

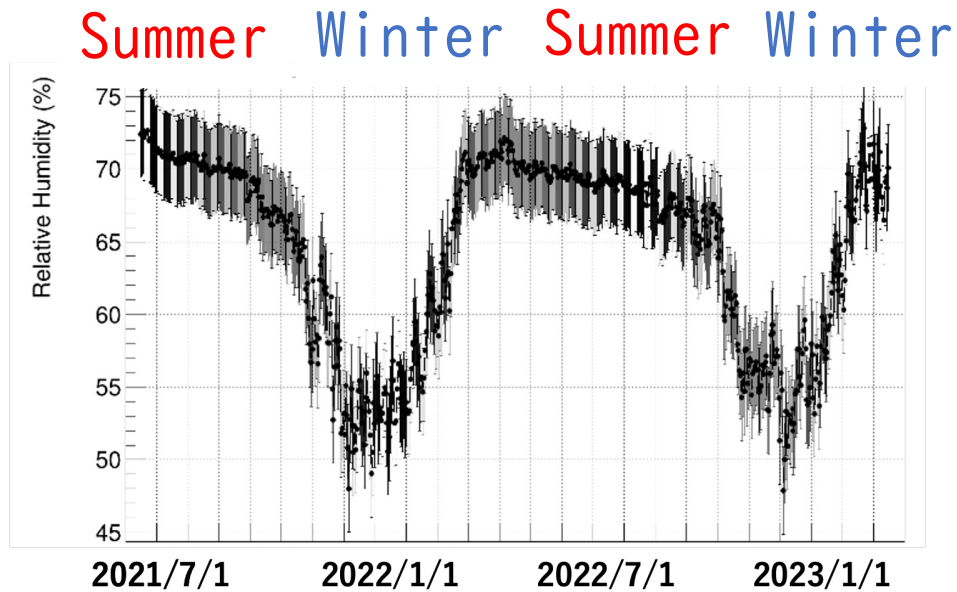


|                         | $R_A$ | $R_B$ | $R_A/R_B$ |
|-------------------------|-------|-------|-----------|
| correlation coefficient | 0.17  | 0.12  | -0.08     |

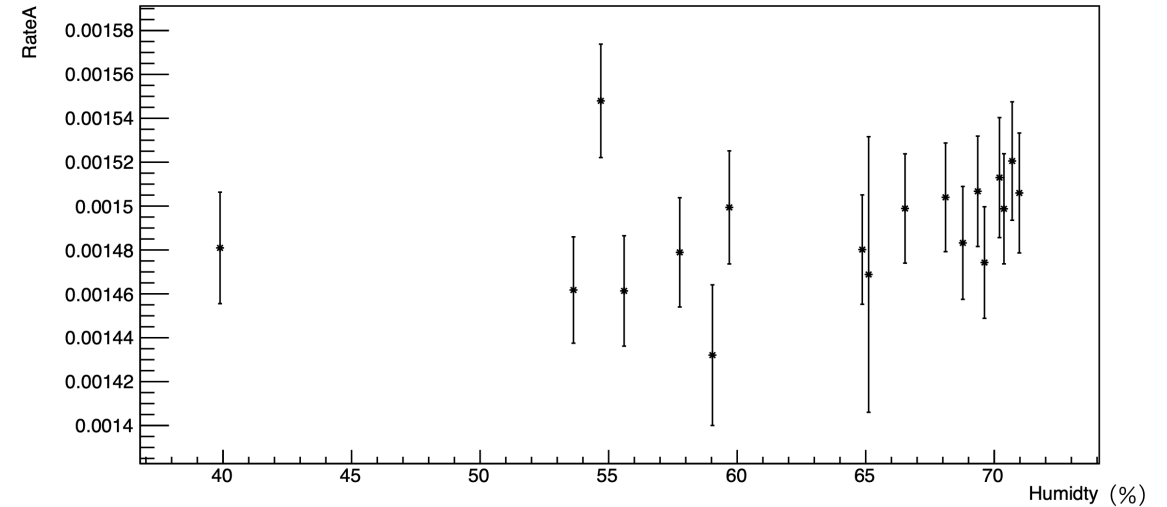
**No correlation**

# Correlation with Humidity in the mine-tunnel air

Humidity in the mine-tunnel air



Scatter plot of  $R_A$  and Humidity

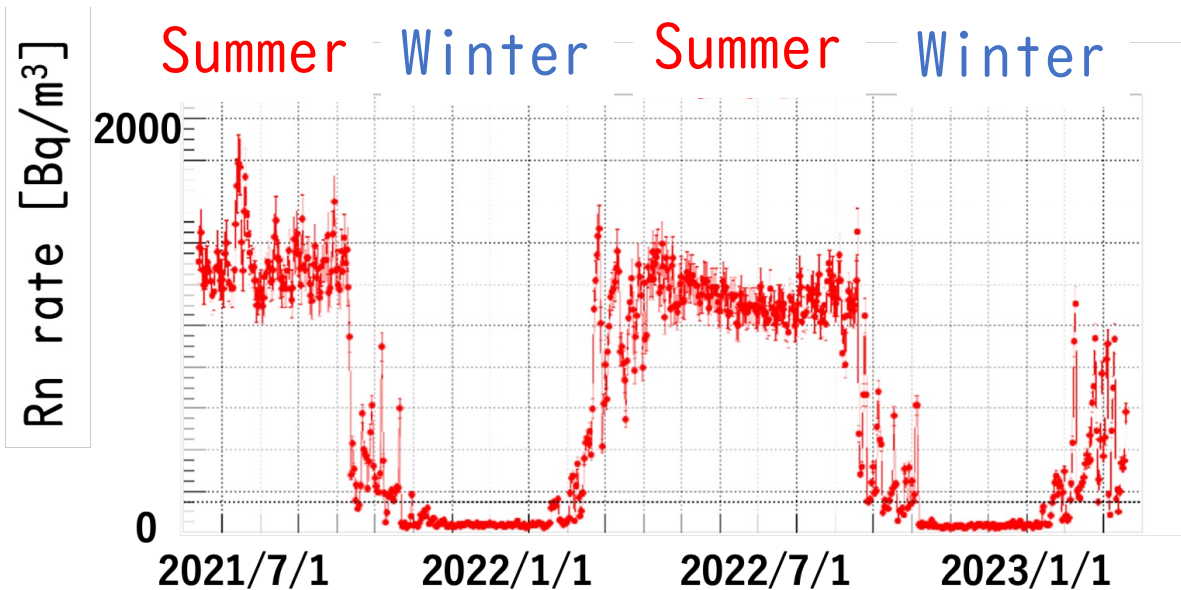


$R_A$ : Weak positive  
 $R_B$ : Weak negative  
 $R_A/R_B$ : Weak positive

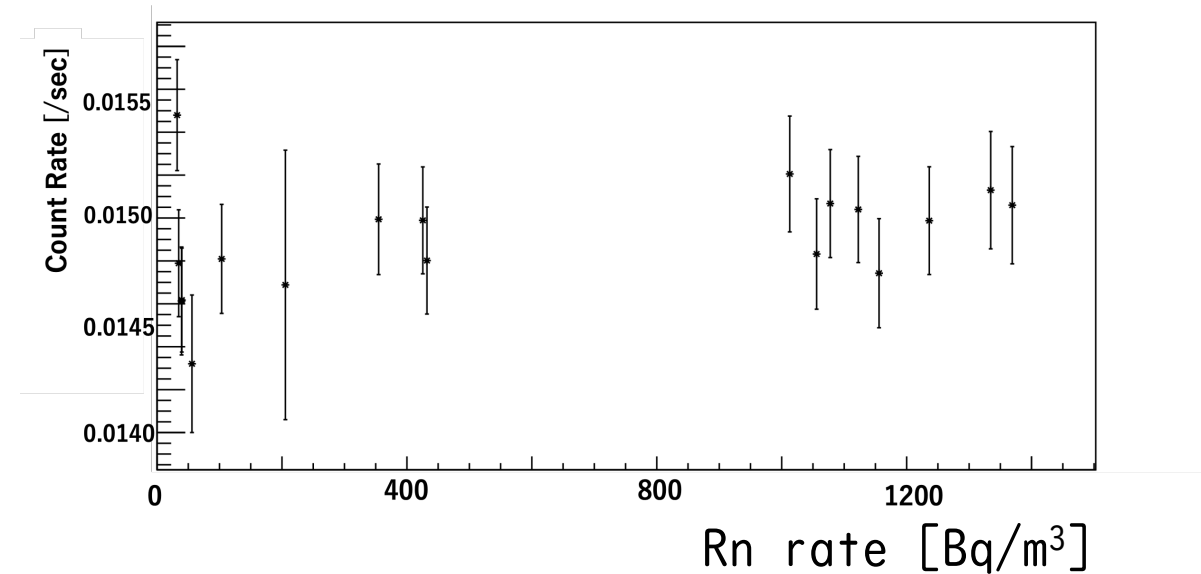
|                         | $R_A$ | $R_B$ | $R_A/R_B$ |
|-------------------------|-------|-------|-----------|
| correlation coefficient | 0.28  | -0.27 | 0.28      |

# Correlation with the Rn rate in the mine-tunnel air

Rn rate in the mine-tunnel air



Scatter plot of  $R_A$  and Rn rate



|                         | $R_A$ | $R_B$ | $R_A/R_B$ |
|-------------------------|-------|-------|-----------|
| correlation coefficient | 0.41  | -0.11 | 0.19      |

$R_A$ : Medium positive  
 $R_B$ : No correlation  
 $R_A/R_B$ : No correlation

# Summary of long-term environmental neutron measurement in the underground

- Conclusion

- No correlation with rainfall
- Weak correlation with humidity in the mine-tunnel air
- Medium correlation with Rn rate in the mine-tunnel air

- ToDo

- Will verify the effects of humidity and Rn rate in the mine-tunnel through simulation

# Liquid scintillator neutron detector

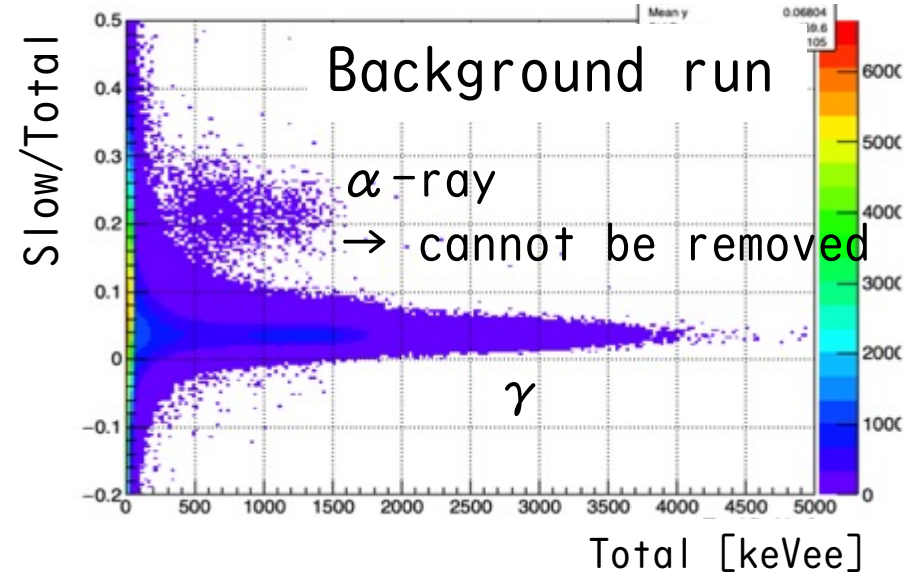
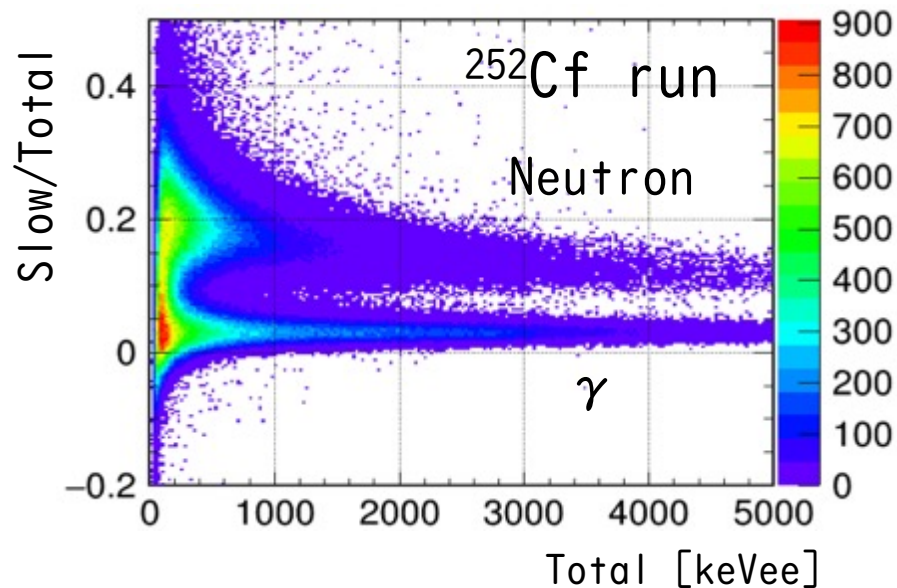
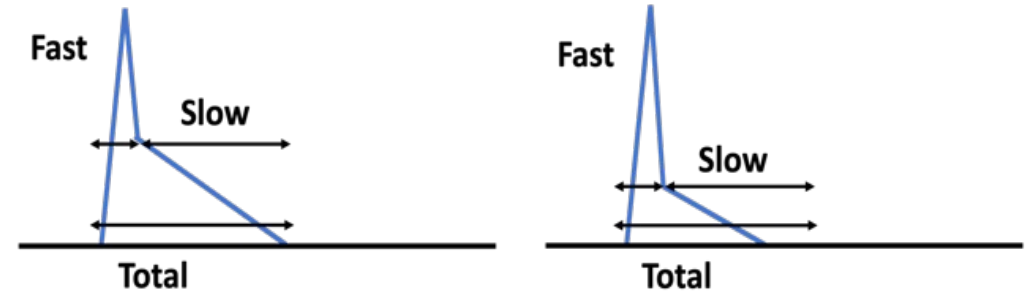


# Liquid scintillator\* neutron detector

- Neutrons are detected through the scattered protons.
- $\gamma$ -rays and electrons can be removed by pulse-shape discrimination, but  $\alpha$ -rays are difficult to remove.

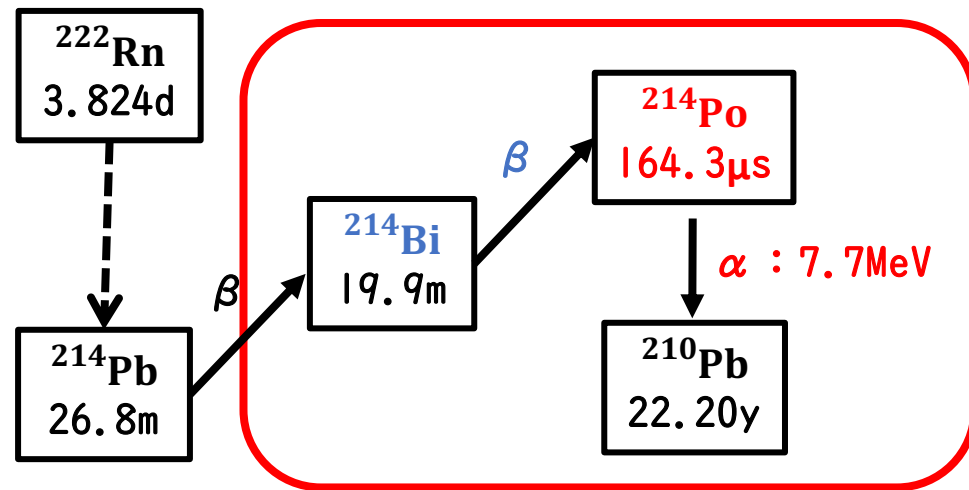
Nuclear event  
(Neutron &  $\alpha$ )

Electron event  
( $\gamma$  &  $\beta$ )



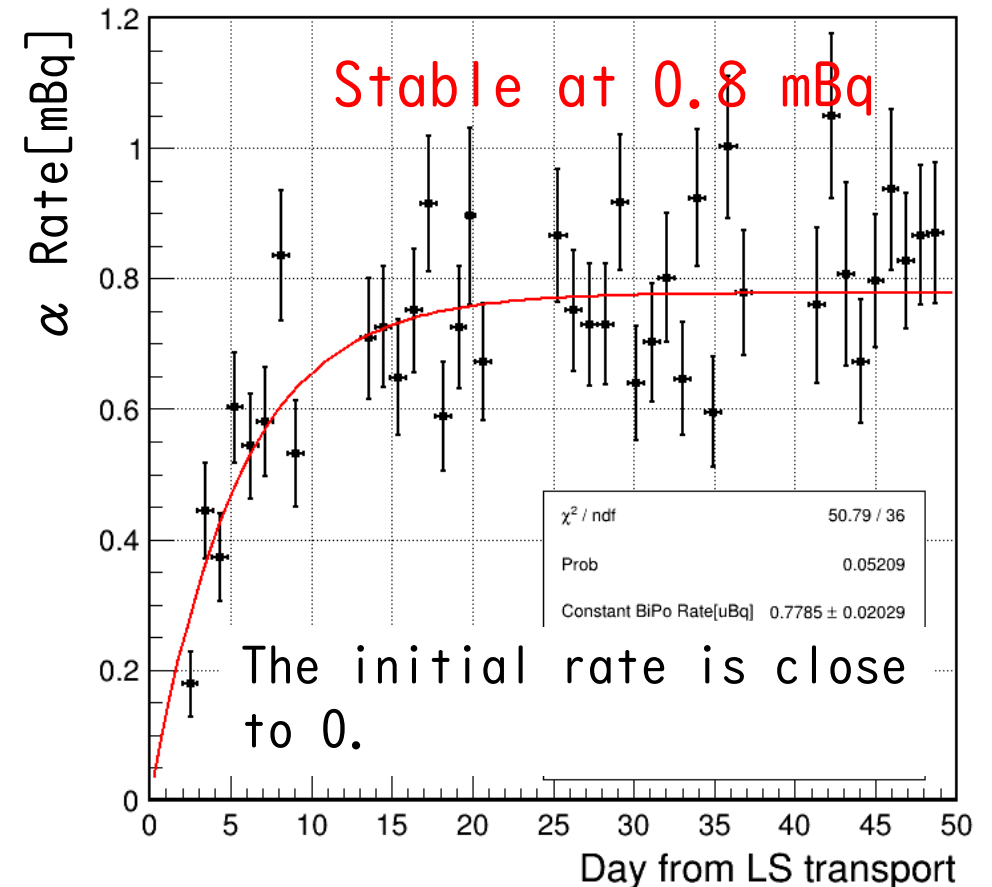
# $\alpha$ -ray background of liquid scintillator detector

- Evaluate  $\alpha$ -ray BG by delayed-coincidence of  $^{214}\text{Bi}$ - $^{214}\text{Po}$



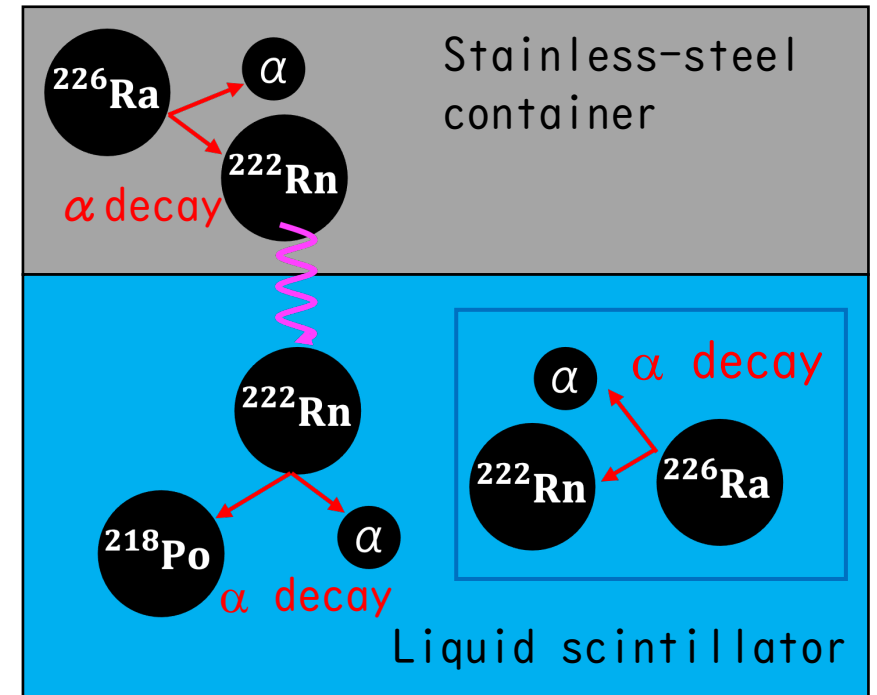
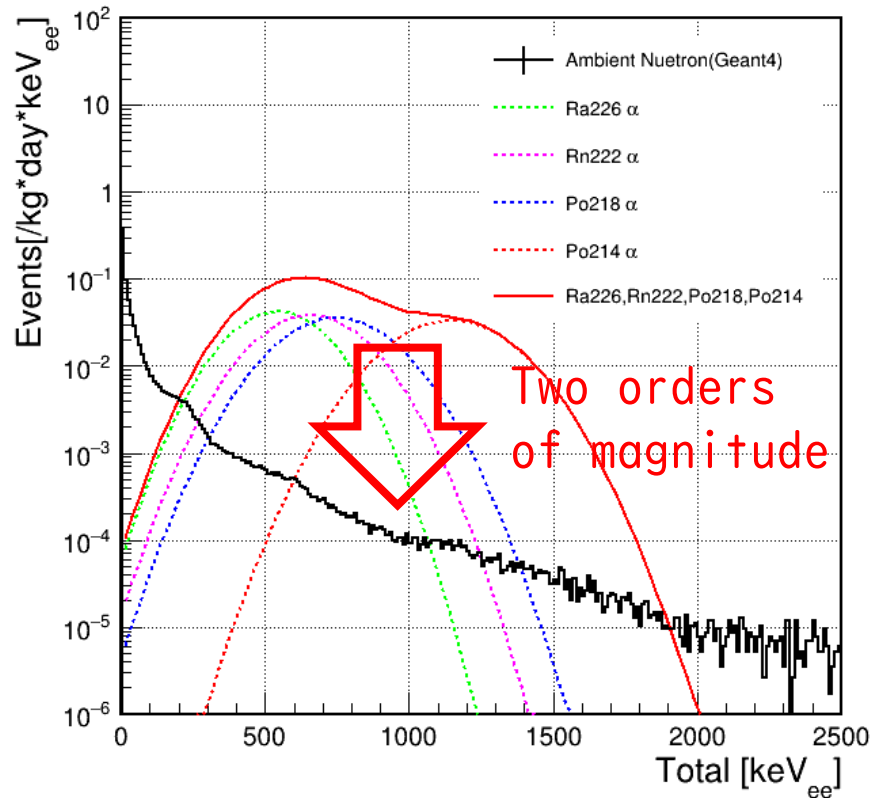
Since the half-life of  $^{214}\text{Po}$  is short,  $^{214}\text{Bi}$ - $^{214}\text{Po}$  can be selected by  $\Delta t$ .

Bi-Po  $\alpha$ -ray rate



# $\alpha$ -ray background of liquid scintillator detector

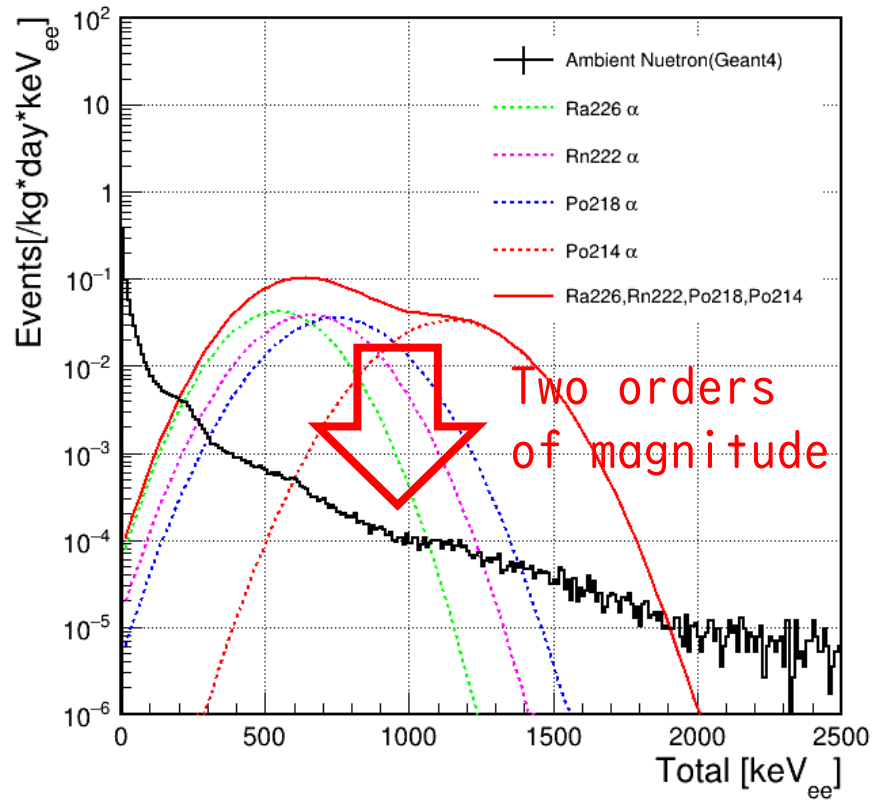
expected neutron signal &  
 $\alpha$   $\alpha$ -ray background (0.8mBq)



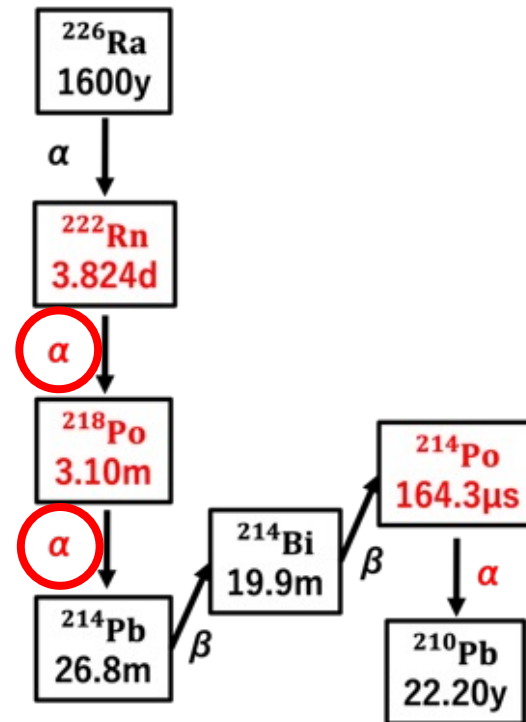
- Reduction by detector improvement ( $\times 1/10$ )
  - Additional purification of liquid scintillator
  - Surface treatment of stainless-steel containers
  - $^{222}\text{Rn}$  reduction by periodic  $\text{N}_2$  bubbling

# $\alpha$ -ray background of liquid scintillator detector

expected neutron signal &  $\alpha$ -ray background (0.8mBq)



- Reduction through analysis ( $\times 1/10$ )
  - Tag the  $\alpha$ -rays from  $^{222}\text{Rn}$  and  $^{218}\text{Po}$  with delayed coincidence measurement.



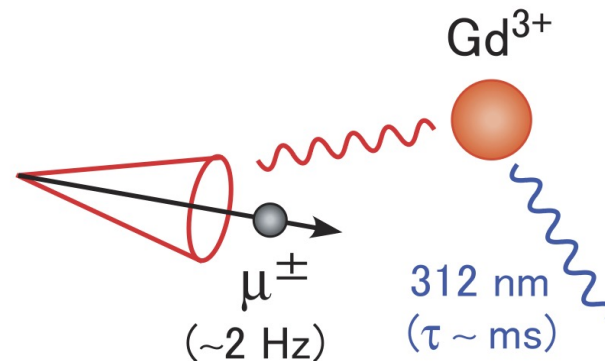
Assuming  $^{222}\text{Rn}$  rate = 0.08 mBq

|                         |         |
|-------------------------|---------|
| Time window             | 500 sec |
| Signal efficiency       | 41.2%   |
| $\alpha$ -ray reduction | 94.4%   |

# Laser-induced luminescence spectroscopy for $\text{Gd}^{3+}$

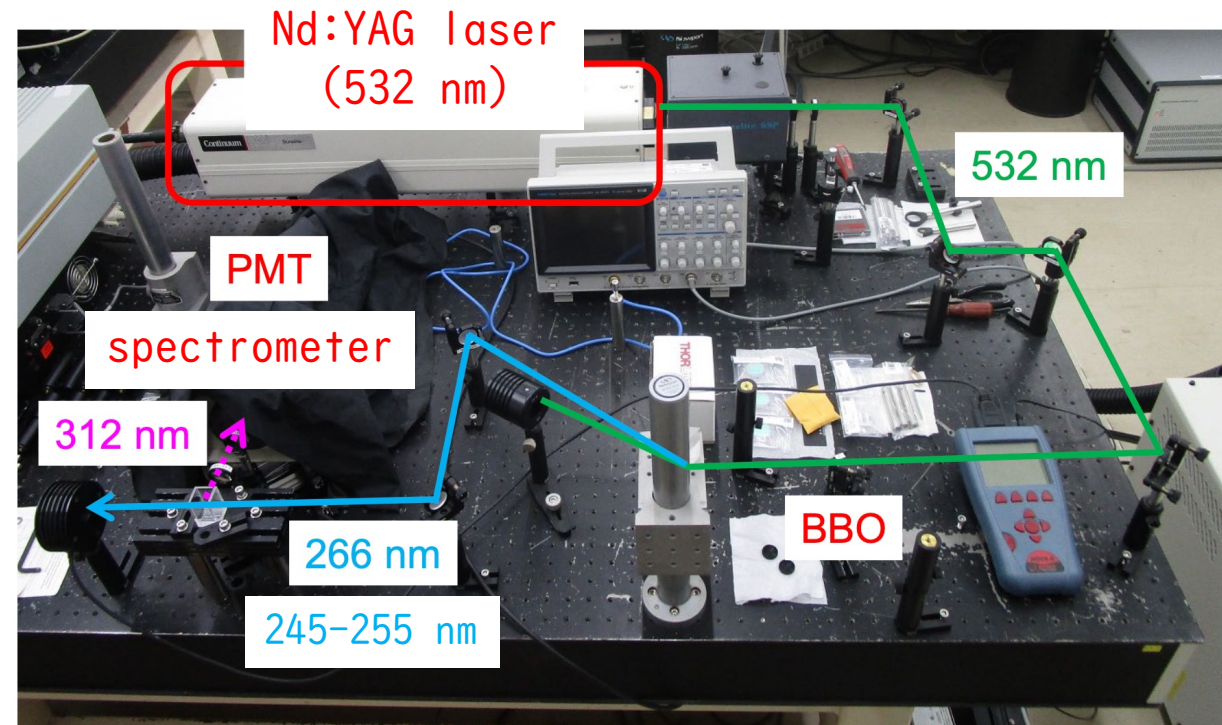
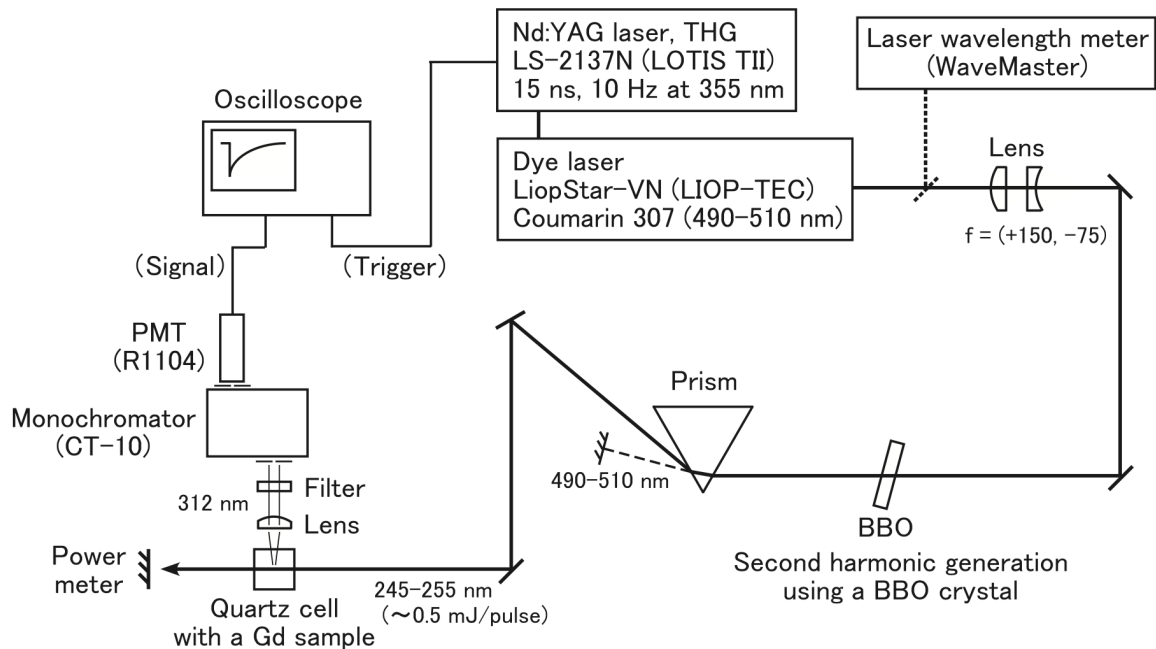
# Laser-induced luminescence spectroscopy for $\text{Gd}^{3+}$

- $\text{Gd}^{3+}$  luminescence is a phenomenon in which  $\text{Gd}^{3+}$  is excited by a photon and emits a 312 nm photon after 0(1) msec.
- In SK-Gd,  $\text{Gd}^{3+}$  luminescence due to a Cerenkov photon could become a background, but there was no detailed measurement of  $\text{Gd}^{3+}$  luminescence in  $\text{Gd}_2(\text{SO}_4)_3$  water.
- We investigated the emission characteristics of  $\text{Gd}^{3+}$  with laser-induced luminescence spectroscopy.

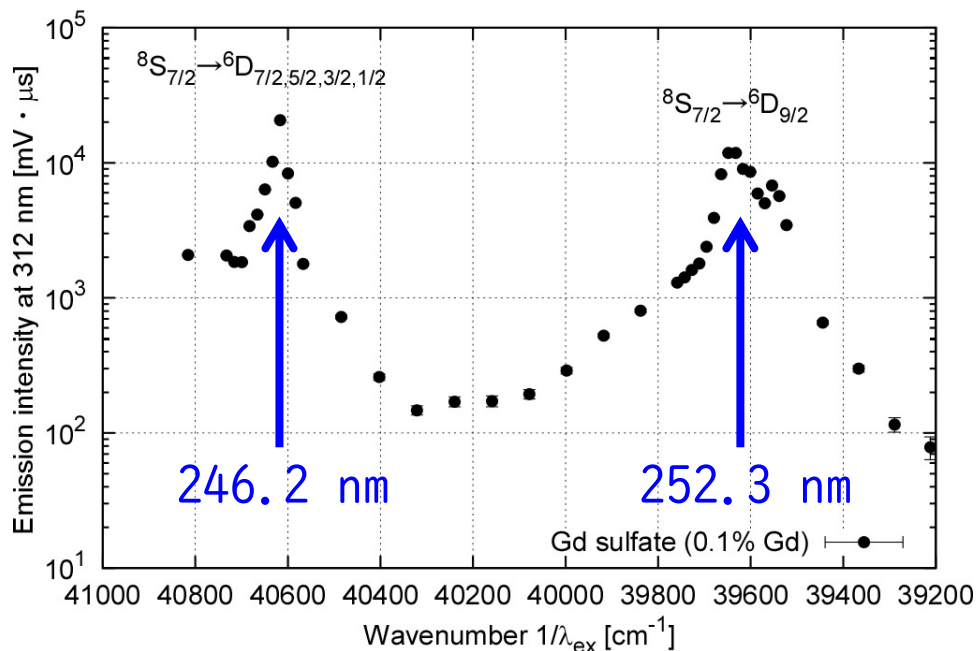
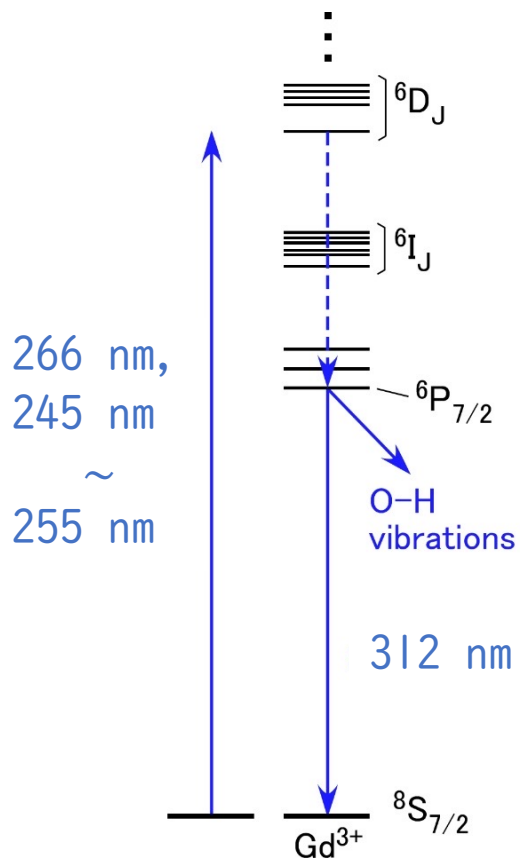


# Laser-induced luminescence spectroscopy for $Gd^{3+}$

266 & 245–255 nm laser is irradiated to the cell w/  $Gd_2(SO_4)_3$  water, and 312 nm photons emitted from the cell are observed with a PMT.

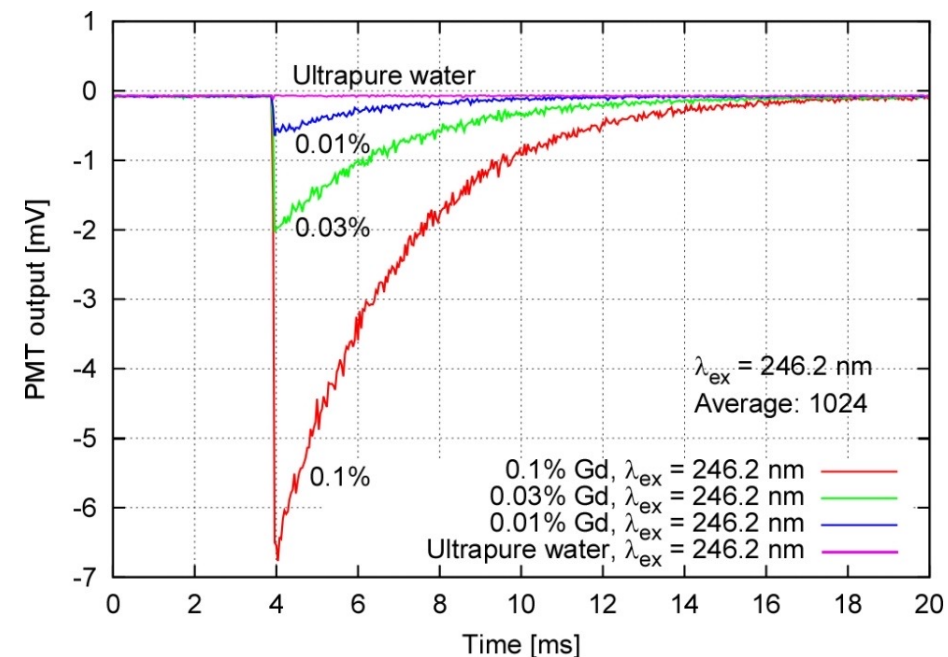


# Laser-induced luminescence spectroscopy for $\text{Gd}^{3+}$



Luminescence increases by two orders of magnitude at resonant wavelength (246.2 nm & 252.3 nm)

246.2 nm laser pulse

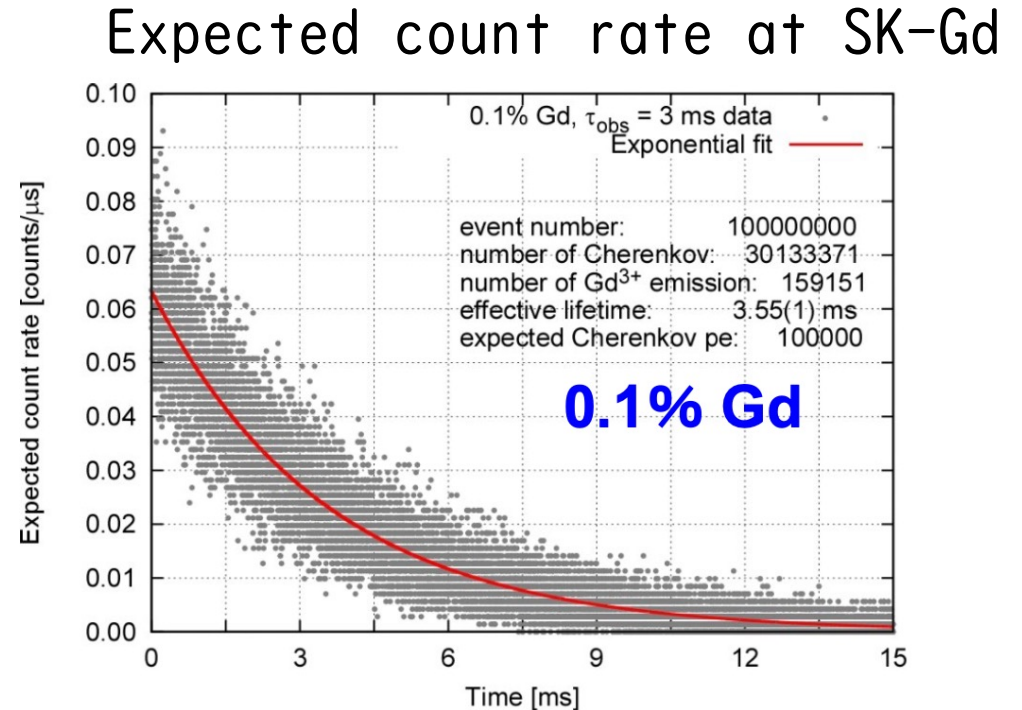
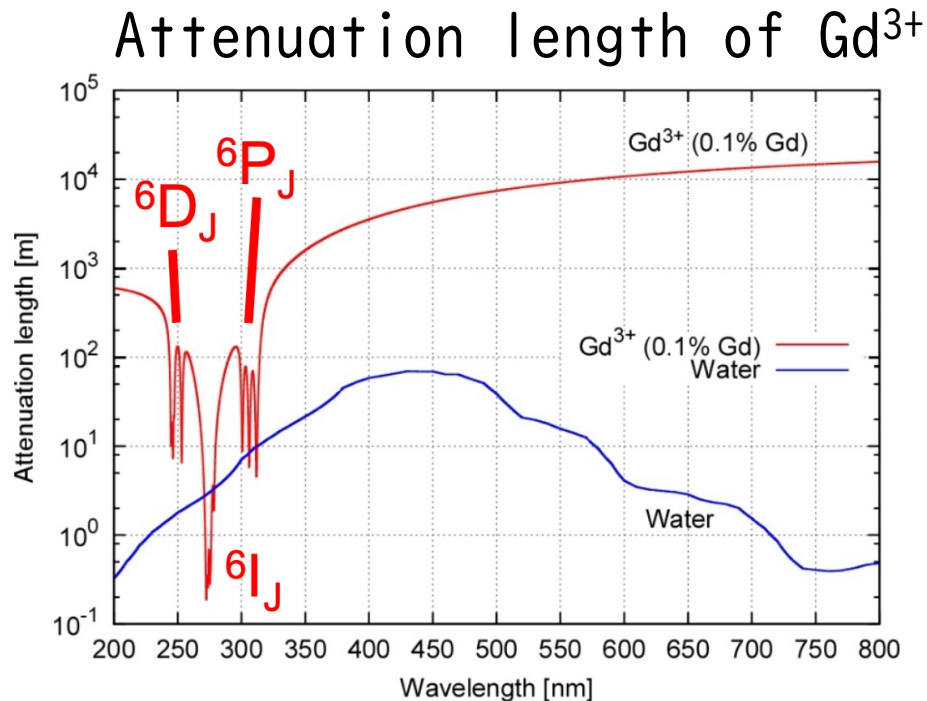


Emission lifetime  $\sim 3$  ms



# Impact of $Gd^{3+}$ luminescence on SK-Gd

A simulation study was performed with SK-Gd geometry.



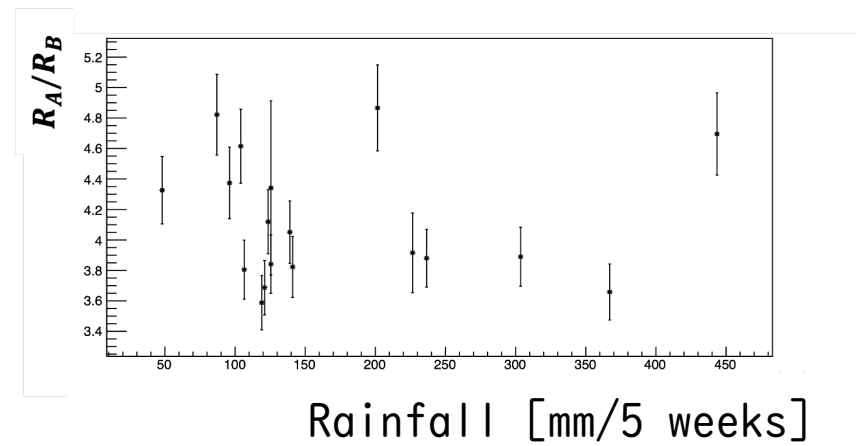
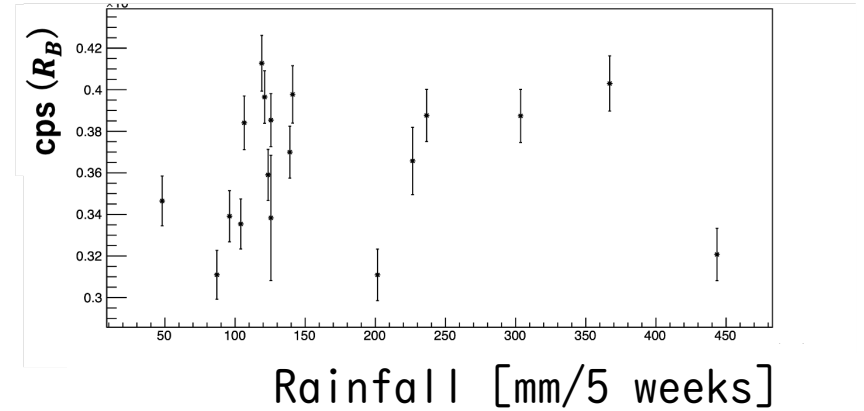
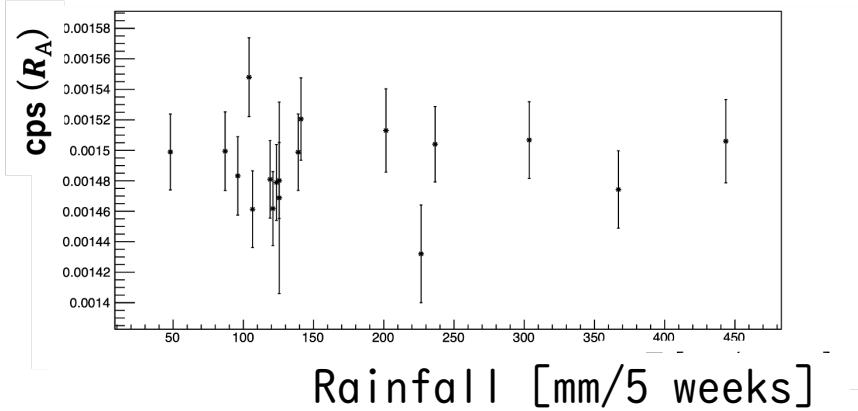
The expected count rate at SK-Gd is  $< 0.1$  counts/ $\mu$ s; therefore, the impact on SK-Gd is small.

# Summary

- Material screenings with HPGe detectors
  - An ultra-low BG HPGe detector with the world's highest level of sensitivity was developed.
- Rn assay in  $\text{Gd}_2(\text{SO}_4)_3$  water
  - The required background level of  $<1 \text{ mBq/m}^3$  is achieved.
- Environmental neutron measurements in the underground
  - Weak correlations with humidity in the mine-tunnel air.
  - Medium correlation with Rn rate in the mine-tunnel air.
- Laser-induced emission spectroscopy for  $\text{Gd}^{3+}$ 
  - The effect on SK-Gd is small.

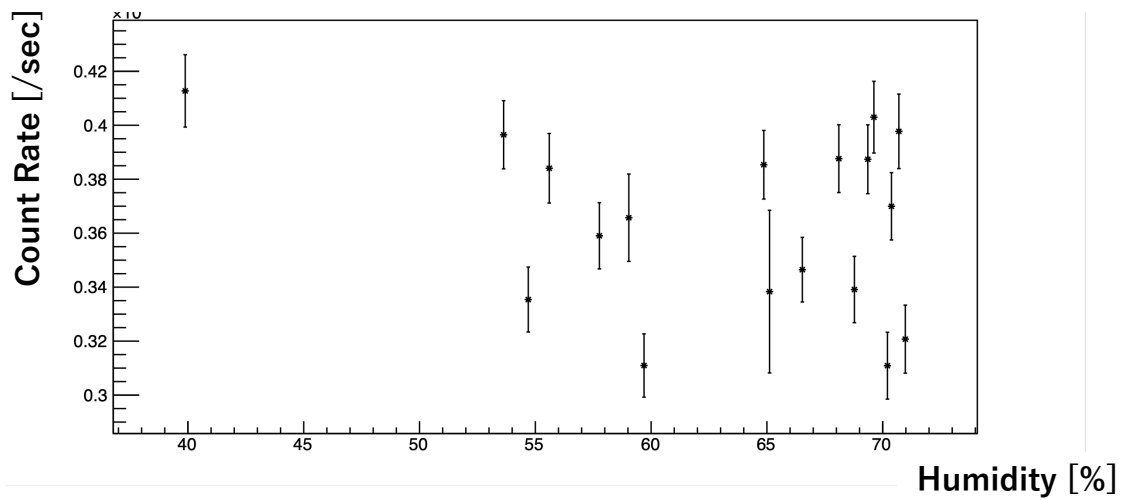
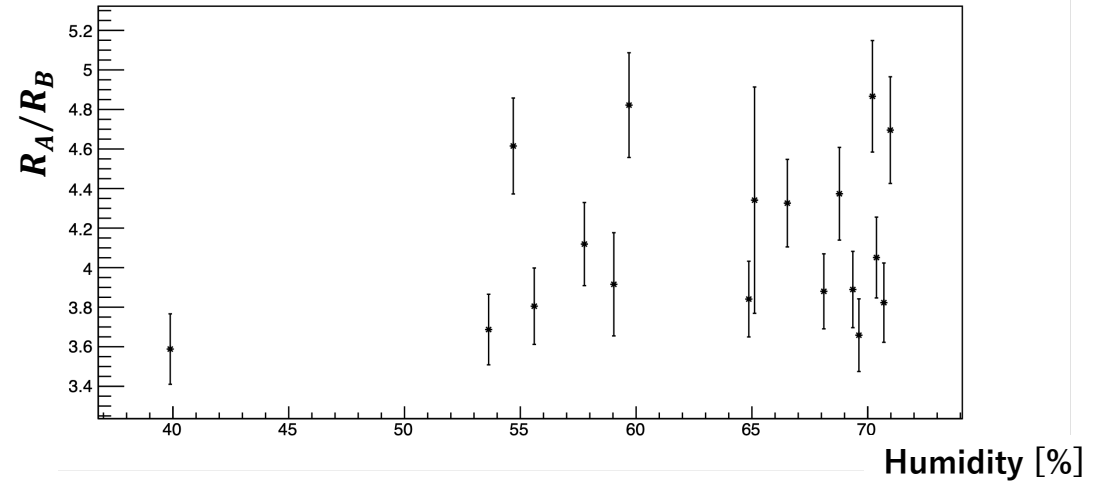
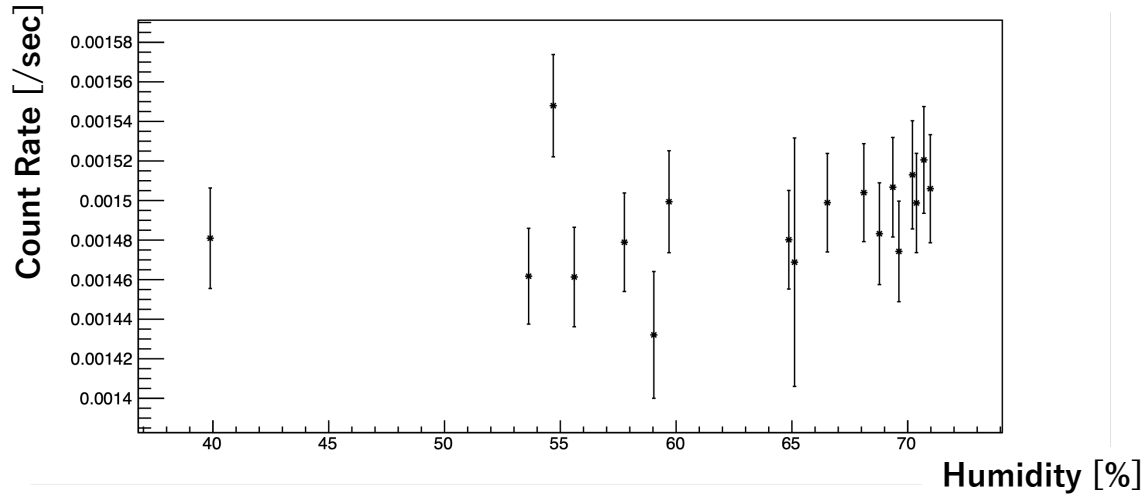
# Backup

# Neutron flux % rainfall



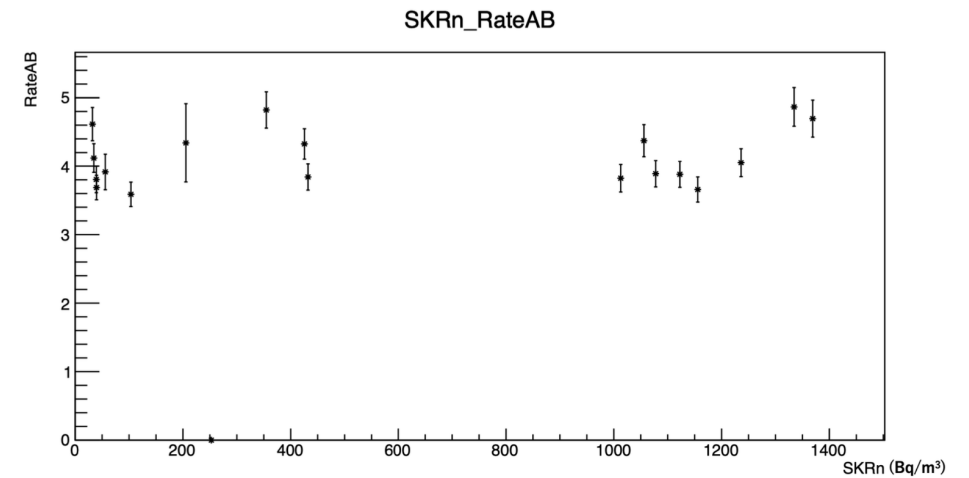
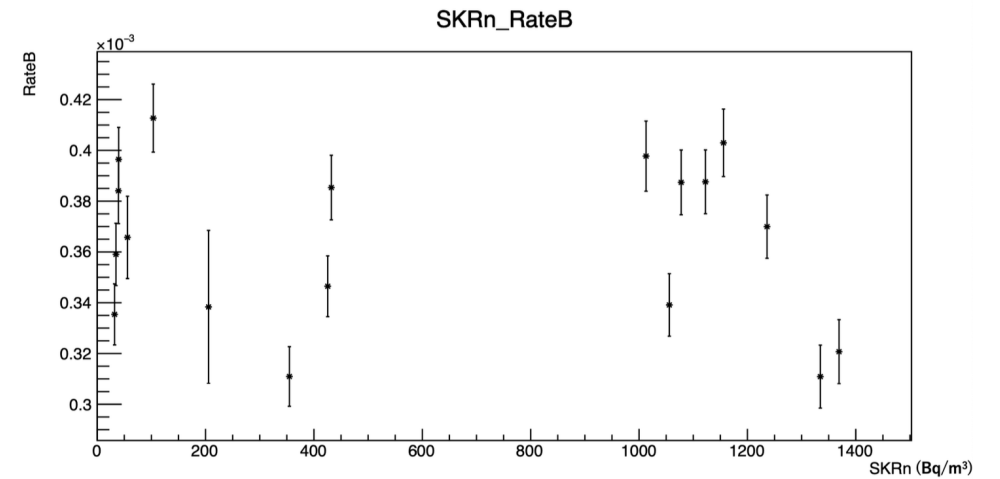
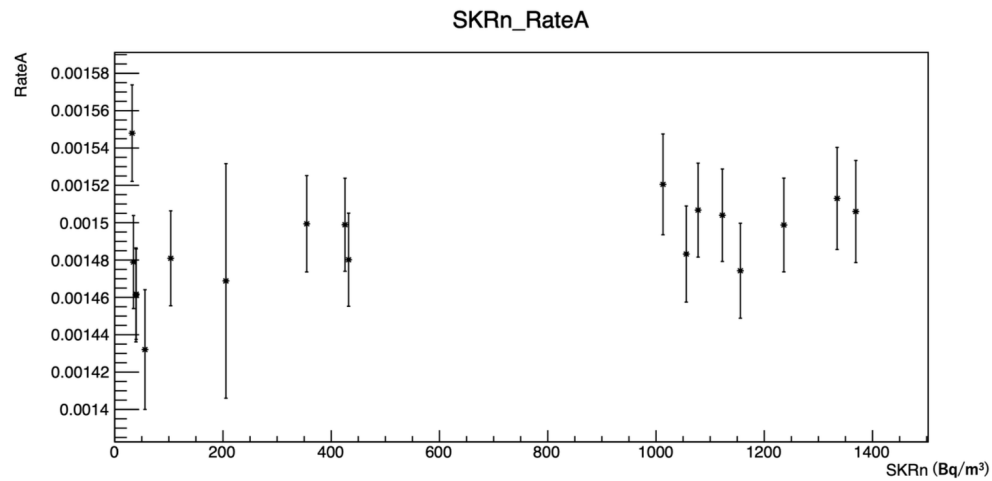
|                         | $R_A$ | $R_B$ | $R_A/R_B$ |
|-------------------------|-------|-------|-----------|
| correlation coefficient | 0.17  | 0.12  | -0.08     |

# Neutron flux % Humidity



|                         | $R_A$ | $R_B$ | $R_A/R_B$ |
|-------------------------|-------|-------|-----------|
| correlation coefficient | 0.28  | -0.27 | 0.28      |

# Neutron flux % Rn rate

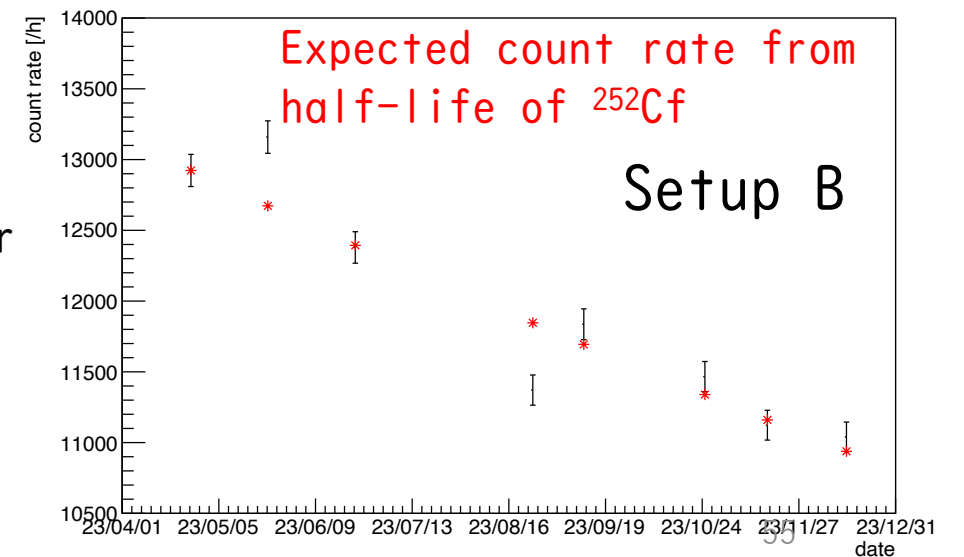
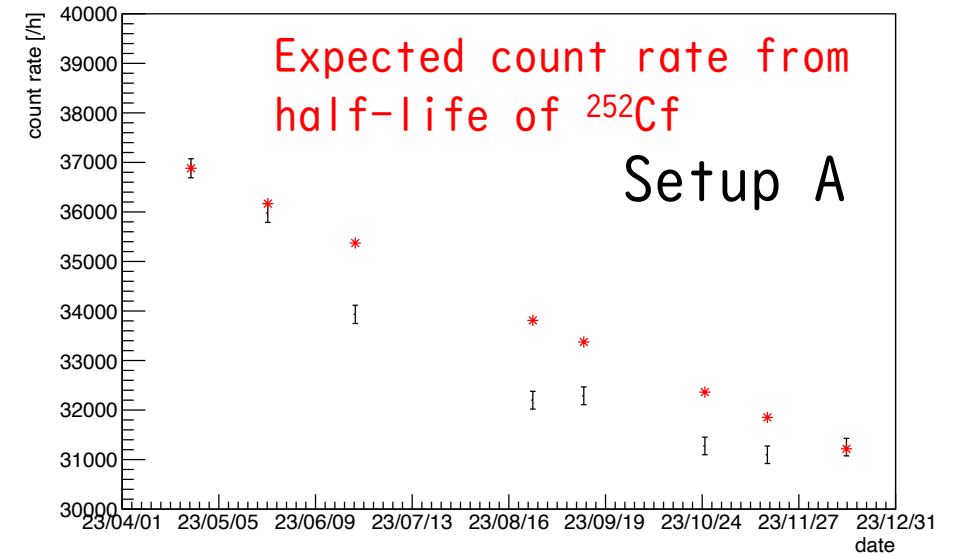
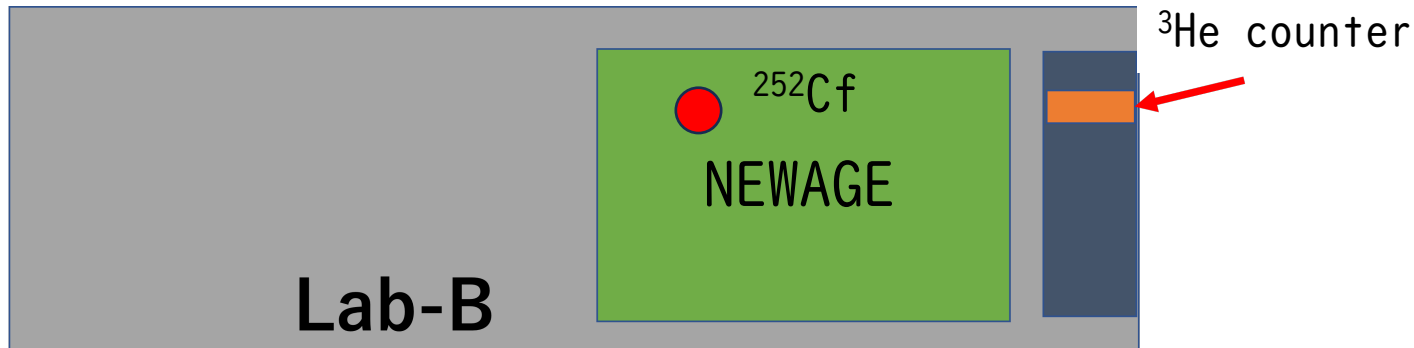


|                         | $R_A$ | $R_B$ | $R_A/R_B$ |
|-------------------------|-------|-------|-----------|
| correlation coefficient | 0.41  | -0.11 | 0.19      |

# Calibration of $^3\text{He}$ proportional counter

Check if the sensitivity of  $^3\text{He}$  proportional counter is stable.

- Started on Apr. 2023
- Irradiation with neutrons from  $^{252}\text{Cf}$  for 1 hour
- Conducted approximately once a month



# Calibration of $^3\text{He}$ proportional counter

The deviation from the expected rate is

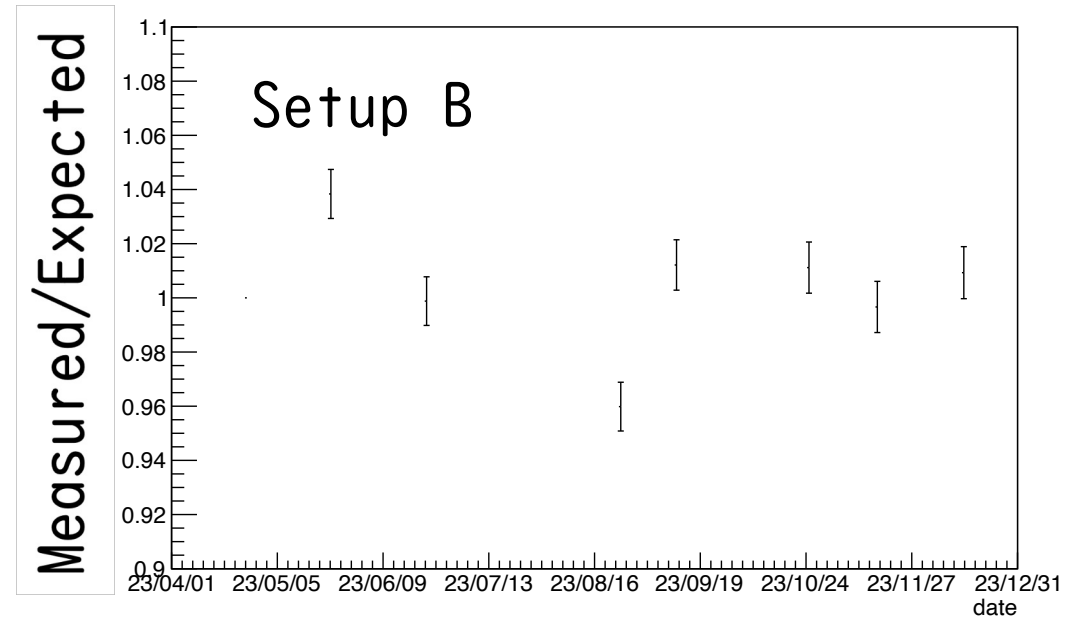
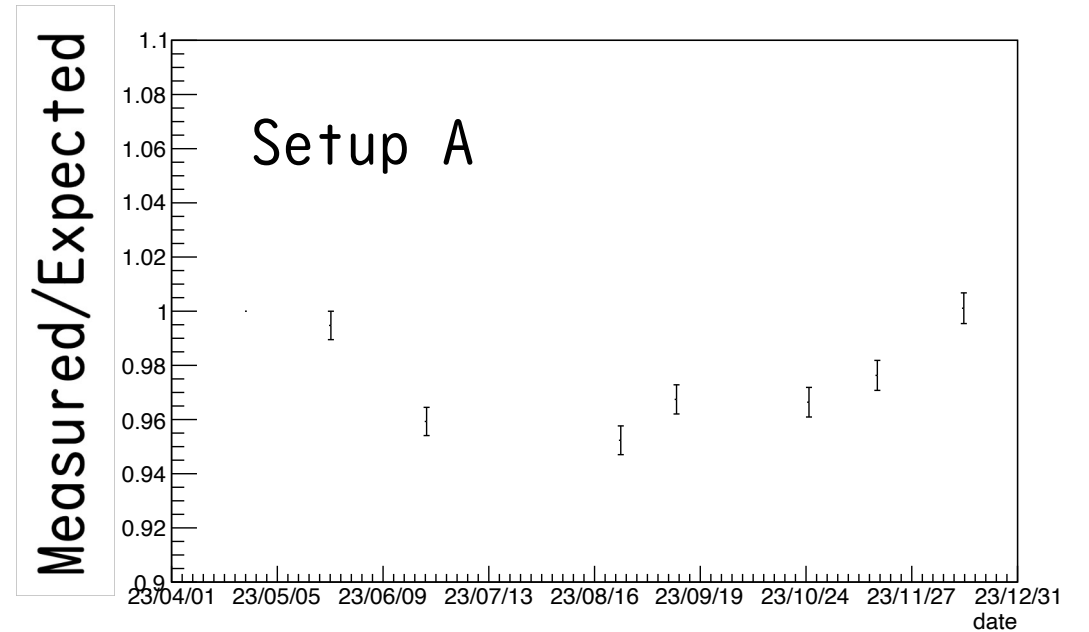
- Setup A:  $-5\% \sim 0\%$
- Setup B:  $-4\% \sim +4\%$

We are currently investigating the cause of the discrepancy from the expected value.

- It has been confirmed that the gain has stayed the same.

Large statistical error

- Considering increasing calibration time





| <b>Coefficient Interval</b> | <b>Correlation</b> |
|-----------------------------|--------------------|
| 0.00 – 0.199                | Very Weak          |
| 0.20 – 0.399                | Weak               |
| 0.40 – 0.599                | Medium             |
| 0.60 – 0.799                | Strong             |
| 0.80 – 1.000                | Very Strong        |